JAN. 2020- APR. 2020 • Volume XXI Number I

THE ASEAN JOURNAL OF RADIOLOGY

Highlight

- Original Article
- Case Report
- Pictorial Essay
- ASEAN Movement in Radiology

Official Journal of ASEAN Association of Radiology

JOURNAL OF RADIOLOGY

ISSN 2672-9393

The ASEAN
Journal of Radiology

CONTENTS

From The Editor

This is the second fully-online-published issue of **The ASEAN Journal of Radiology** telling us not only scientific works but also interesting movements in radiology in ASEAN countries. The establishment of a new sonographer system in Thailand has been recorded in this issue.

The ultimate goal of medical radiology, like other subjects in health science, is to promote health, detection and treatment of diseases for the public. The ASIAN Intensive Reader of Pneumoconiosis (AIR Pneumo) project is upgrading the skill in interpreting chest radiographs of dust-exposed workers, based on the ILO classification system, in physicians in Asian nations. The project includes standardization, examination, certification, and recertification every 5 years to guarantee quality and consistency of the skill in interpretation. The story of this project is revealed in this copy.

Scientific works provide us data, information, or facts which are very close to the truth by minimizing distortion. To do so, researchers need to know how to select the materials and how to choose the method of measurement or display to reveal the answer they want. To publish their works, a good reviewing system and qualified reviewers are indispensable. We receive active participations from many reviewers, mainly in Thailand. We welcome and are attempting to invite reviewers in all subspecialties in radiology from all countries in ASEAN to qualify articles published in our journal.

Wiwatana Tanomkiat, M.D.
Editor,
The ASEAN Journal of Radiology
Email: aseanjournalradiology@gmail.com

Original Article

Value of computed tomography angiographic collateral status in prediction of malignant middle cerebral artery infarction

Sasitorn Petcharunpaisan, M.D.[(1)]
Wannaporn Ngernbumrung, M.D.[(1)]
Sukalaya Lerdlum, M.D.[(2)]
From [(1)]Department of Radiology, King Chulalongkorn Memorial Hospital, The Thai Red Cross Society, Bangkok, Thailand.
[(2)]Department of Radiology, Faculty of Medicine, Chulalongkorn University, Bangkok, Thailand.
Address correspondence to S.P. (e-mail: sasitorn.pe@chulahospital.org)

Abstract

Objective: To determine whether the collateral status evaluated by single phase computed tomographic angiography (CTA) helped prediction of Malignant middle cerebral artery infarction (mMCAi) in patients with large arterial occlusion who did not receive endovascular treatment.

Materials and Methods: We retrospectively reviewed patients with acute is chemic stroke in anterior circulation in our institute from January 2015 to December 2015. We analyzed clinical data, baseline National Institutes of Health Stroke Scale (NIHSS), Alberta Stroke Program Early CT Score (ASPECTS) on baseline nonenhanced computed tomography of the brain (NECT brain), and CTA collateral status. " mMCAi" was defined based on clinical criteria.

Results: Thirty-five patients were included. The mean age was 68.8±15.56 years. The mean baseline NIHSS and baseline ASPECTS were 17(±5) and 6(±3), respectively. All patients received intravenous thrombolysis. CTA collateral status and baseline NECT ASPECTS were significantly correlated with development of mMCAi (P-value = 0.007 and 0.001). Only baseline NECT ASPECTS was an

independent predictive factor for mMCAi (OR 0.63, 95%CI 0.46-0.86, P-value =0.004). Patients with baseline NECT ASPECTS ≤ 7 were more likely to develop mMCAi (OR 14.29 95%CI 1.57-129.94, P-value 0.018).
Conclusion: In times of acute stroke, patients with proximal MCA or ICA occlusion received intravenous thrombolysis alone, baseline NECT ASPECTS and CTA collateral status were significantly correlated with development of mMCAi. However, only baseline ASPECTS ≤ 7 was an independent predictor for mMCAi.

Keywords: CTA collateral status, Malignant MCA infarction, NECT ASPECTS, Acute ischemic stroke.

Introduction

Stroke is one of the leading causes of death and disability worldwide. Large cerebral infarction due to occlusion of middle cerebral artery (MCA) can be a life-threatening condition. Acute infarction involving a large portion of cerebral hemisphere with associated space-occupying cerebral edema, leading to rapid neurological deterioration has been termed "malignant MCA infarction (mMCAi)" [1,2]. Brain edema with a subsequent midline shift, brain herniation and increased intracranial pressure (ICP) may lead to coma and death. Significant space occupying effect usually manifests between the second and the fourth days after stroke onset; however, it possibly occurs more rapidly within 24 hours [1,2]. Up to eighty percent of patients with mMCAi treated with conservative medical therapy alone developed coma and death within 2 to 5 days. Surviving patients were left with severe disability and poor quality of life. Early treatment with decompressive surgery (hemicraniectomy) could reduce ICP, extensive brain edema and further infarction when performed within 48 hours after stroke onset [3]. Decompressive craniectomy not only reduces mortality, but also improves functional outcome and reduces longstanding critical care therapy. Thus, it is important to identify predictors of mMCAi which may help in management planning [3-6].

Cerebral collateral circulation is necessary to maintain cerebral blood flow and penumbra when cerebral arterial insufficiency due to thromboembolism, hemodynamic disturbance or a combination occurs [7,8]. Baseline collateral status is correlated with baseline infarct volume and infarct growth over 24 hours [9]. Recent studies demonstrated effect modification by collateral status on relationship between recanalization and good clinical outcome [9,10]. Collaterals impact efficacy and safety of endovascular treatment in acute ischemic stroke patients; patients with more robust collateral circulation had better recanalization, reperfusion and functional outcomes, as well as lower periprocedural symptomatic intracranial hemorrhage and mortality [10-16]. In these recent years, assessment of collateral circulation with multiphase CTA showed advantages over single phase CTA giving information on the degree and extent of pial arterial filling in a time resolved manner and has been used in The Endovascular Treatment for Small Core and Anterior Circulation Proximal Occlusion with Emphasis on Minimizing CT to Recanalization Times (ESCAPE) trial as a criterion for patient selection to endovascular treatment [17,18].

Recent studies found that collateral circulation, assessment with both single phase and multiphase CTA, is one of the factors that independently predict malignant MCA infarction, together with baseline NIHSS, NECT ASPECTS and revascularization status [4,7,19]. Then we sought to determine whether CTA collateral status derived from single phase CTA may help prediction of mMCAi in acute stroke patients with large arterial occlusion who did not receive endovascular treatment.

Materials and methods

Patients

We retrospectively reviewed patients with acute ischemic stroke in anterior circulation who underwent stroke fast tract imaging protocol in our institute from January 2015 to December 2015. Our stroke fast tract imaging protocol included NECT brain, CTA of the brain and neck and CT brain perfusion. The inclusion criteria were: 1) patient's age was 18 years old or above; 2) the onset of symptoms at the time performing fast tract image protocol was lower than 6 hours; 3) there was the presence of large arterial occlusion (internal carotid artery (ICA) or M1 segment of MCA) on CTA; 4) patient did not receive endovascular treatment; 5) patients may or may not receive intravenous administration of recombinant tissue-type plasminogen activator (rtPA). Exclusion criteria included: 1) the presence of intracranial hemorrhage on NECT; 2) the presence of previous large cerebral infarction in ipsilateral cerebral hemisphere or other intracranial space taking lesion on NECT; 3) poor image quality.

Patients' clinical information were collected from the hospital information system and outpatient records, including demographic data, clinical presentation, the onset of symptoms, onset-to-image time, NIHSS score, information of rtPA administration, and records of conscious deterioration and craniectomy during admission.

CT imaging protocol

All scans were obtained using 64 slice multidetector CT scanner installed at emergency department (Brilliance 64 Philips Health-care, Netherland). Parameters of NECT scan are as follows; a detector collimator of 64x0.4 mm, tube current of 300 mA, tube voltage of 120 kV, and FOV of 25 cm, covering from foramen magnum to the vertex. Axial image with 5-mm slice thickness was transferred to pictures achieving and information system (PACS). Parameters of CTA are as follows; detector collimation of 64 x 0.6 mm, tube current of 400 mA, tube voltage of 120 kV, and field of view of 50 cm, covering from aortic arch up to vertex. Acquisition was triggered using a bolus tracking (100 HU) in the aortic arch after 80 mL of intravenous contrast medium (Ultravist® 300) injection with

an injection rate of 4 mL/s, followed by 40 mL saline flush. One-millimeter-thick axial maximal intensity projection (MIP) image, together with 8-millimeter-thick MIP image in axial, coronal and sagittal planes are transferred to PACS as routine image reconstruction protocol.

Image analysis

All CT images were reviewed by two readers (reader 1 was a second year neuroradiology fellow and reader 2 was a neuroradiologist with 8-year experience in neuroimaging). The two readers were blind to clinical information, NECT and CTA results in each patient.

Baseline ASPECTS (Alberta Stroke Program Early CT Score) was evaluated on the initial axial 5-millimeter-thick NECT brain. CTA collateral status was evaluated on 8-millimeter-thick axial MIP images of CTA, using CTA collateral score derived from PROACT (Prolyse in Acute Cerebral Thromboembolism Trial) investigators with a scale of 0-3. According to this score, collaterals were defined as contrast filling pial arteries beyond the occluded site with different degrees on scale 0-3 as follows; 0 = absent collaterals supply to the occluded MCA territory; 1 = collaterals filling ≤ 50% of the occluded territory; 2 = collaterals filling > 50%, but <100% of the occluded territory; 3 = collaterals filling = 100% of the occluded territory. Score 0-1 defined poor collaterals and score 2-3 defined good collaterals.

"mMCAi" was defined when there were clinical records of decreased in the level of consciousness to give a score of 1 or more on item 1a of the NIHSS, according to ECASS (European Cooperative Acute Stroke Study) investigators [4, 5]. Hemorrhagic transformation was defined and graded as follows: HI type 1 (HI-1) = small heterogeneous petechiae along the margins of the infarct; HI type 2 (HI-2) = more confluent heterogeneous petechiae within the infarcted area; PH type 1 (PH-1) = homogeneous hematoma covering ≤ 30% of the infarcted area with mild space-occupying effect; PH type 2 (PH-2) = dense hematoma > 30% of the infarcted area with significant space-occupying effect. (HI = hemorrhagic infarction, PH = parenchymal hemorrhage). Only PH-2 was defined as symptomatic hemorrhagic transformation [20].

Statistical analysis

Patients were divided into mMCAi and non-mMCAi groups. Categorical variables were expressed in number (%) and the continuous variable as the mean standard deviation. The 2 groups were compared for demographic categorical variables with the independent-sample T-test for continuous parameters and Chi-square test for categorical variables. Logistic regression was used to compute unadjusted and multivariable-adjusted odds ratios (OR) for the dichotomous outcomes (poor and good collateral status) of the mMCAi or non-mMCAi groups.

OR was presented with the associated 95% confidence intervals (CI). The threshold for statistical significance was set at $p < 0.05$. All statistical analyses were performed using the Statistical Package for the Social Sciences software version 16 (SPSS). Kappa statistics was made on the interrater agreement for CTA collateral score, baseline ASPECTS and symptomatic hemorrhagic transformation. The limits for Kappa statistics were the following; 0.4-0.6, moderate agreement; 0.6-0.8, good agreement; >0.8, excellent agreement.

Results

Thirty-five patients (19 women, 16 men; the mean age, 68.8 years±15.56) fulilling all inclusion criteria, were selected. Twelve (34%) patients developed mMCAi, whereas 23 patients (66%) did not (non-mMCAi). All patients received intravenous rtPA therapy. Baseline characteristics of mMCAi and non-mMCAi patient groups were shown in Table 1.

Table 1: *Baseline characteristics*

	mMCAi (n =12, 34%)	non-mMCAi (n= 23, 66%)	Total	P-value
Age, y, mean (SD)	71.42 (±10.33)	67.13 (±17.73)	68.6 (±15.56)	0.37
Female, n,%	6 (50%)	13 (57%)	19 (54%)	0.73
Cardiovascular risk factors				
DM, n,%	2 (17%)	4 (17%)	6 (17%)	1
HT, n,%	4 (33%)	9 (39%)	13 (37%)	1
AF, n,%	0 (0%)	2 (9%)	2 (6%)	0.53
DLD, n,%	2 (17%)	5 (22%)	7 (20%)	1
Onset, hours, mean (SD)	2.84 (±1.3)	2.95 (±1)	2.91 (±1.1)	0.8
Baseline NIHSS score, mean (SD)	18 (±7)	17 (±5)	17 (±5)	0.54
Baseline ASPECTS, mean (SD)	4 (±2)	7 (±2)	6 (±3)	0.001*
Collateral status				0.007*
Poor (<2), n,%	12 (100%)	13 (57%)	25 (71%)	
Good(≥2), n,%	0	10 (43%)	10 (29%)	

Note:- *DM indicates diabetes mellitus; HT, hypertension; AF, atrial fibrillation; DLD, dyslipidemia; NIHSS, National Institutes of Health Stroke Scale; ASPECTS, Alberta Stroke Program Early CT Score; mMCAi, malignant middle cerebral artery infarction.*

Only one patient developed symptomatic intracranial hemorrhage (PH-2). The mMCAi group had a significantly lower mean baseline ASPECTS compared to non-mMCAi group 4(±2) versus 7(±2), P-value = 0.001. Collateral status was significantly correlated with development of mMCAi, P-value = 0.007. None of patients with good collateral score developed mMCAi (0 versus 10). On the other hand, other baseline clinical characteristics, including NIHSS, were not different among the two groups.

In multivariate analysis, baseline ASPECTS was an independent predictive factor for mMCAi (OR 0.63, 95%CI 0.46-0.86, P-value =0.004). Patients with baseline ASPECTS ≤ 7 were more likely to develop mMCAi (OR 14.29 95%CI 1.57-129.94, P-value 0.018). On the other hand, collateral status evaluated by single phase CTA was not an independent predictor of mMCAi.

We did not find the correlation between clinical and imaging characteristics and development of symptomatic hemorrhagic transformation. (Table 2 and 3)

Table 2: *Prediction of mMCAi: multivariate binary regression analysis*

	OR	95%CI	P-value
Baseline NIHSS	1.04	0.91-1.19	0.53
Baseline ASPECTS	0.63	0.46-0.86	0.004*
Collateral status	0.81	0.07-8.91	0.86
Baseline ASPECTS≤7	14.29	1.57-129.94	0.018*

Note: *CI, confidence interval; OR, odds ratio.*

Table 3: Prediction of symptomatic hemorrhagic transformation (PH2): multivariate binary regression analysis

	OR	95%CI	P-value
Baseline NIHSS	1.03	0.69-1.53	0.87
Baseline ASPECTS	0.68	0.29-1.64	0.40
Collateral Status	0.43	0.01-19.4	0.66
Baseline ASPECTS≤7	1.26	0.68-2.33	0.45

Note:- *CI indicates confidence interval; OR, odds ratio.*

There was an excellent interrater agreement for CTA collateral grading (1.0). Interrater agreement for baseline NECT ASPECTS and hemorrhagic transformation were good (0.71) and excellent (0.86), respectively. Some examples of cases are shown in Figure 1 and Figure 2.

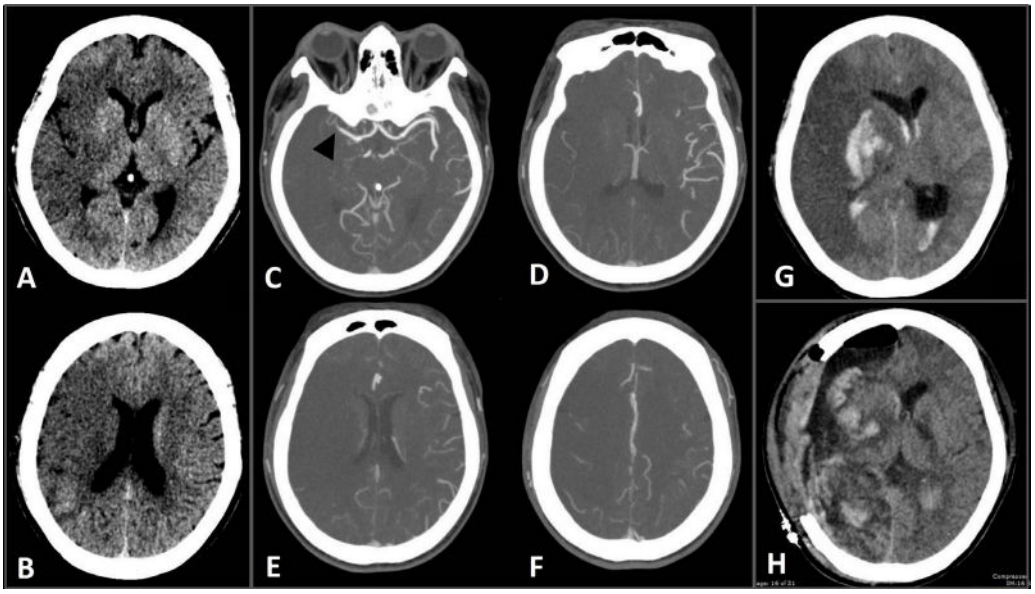

Figure 1. A *52-year-old female with acute right MCA infarction. Baseline NECT at 3 hours after onset (A and B) showed large hypodensity change in right cerebral hemisphere, ASPECTS = 1. Eight-mm axial MIP CTA (C-F) showed occlusion at right distal M1 (black arrowhead in C) with poor collaterals, score = 1; collaterals filling ≤ 50% of the occluded territory. Follow up NECT at 24 hours (G) showed large edematous infarction with hemorrhagic transformation in right basal ganglia extending to lateral ventricles, midline shift and hydrocephalus. Decompressive craniectomy was done and follow up NECT at 24 hours (H) showed less degree of midline shift and improved hydrocephalus. New infarction in left globus pallidus was noted.*

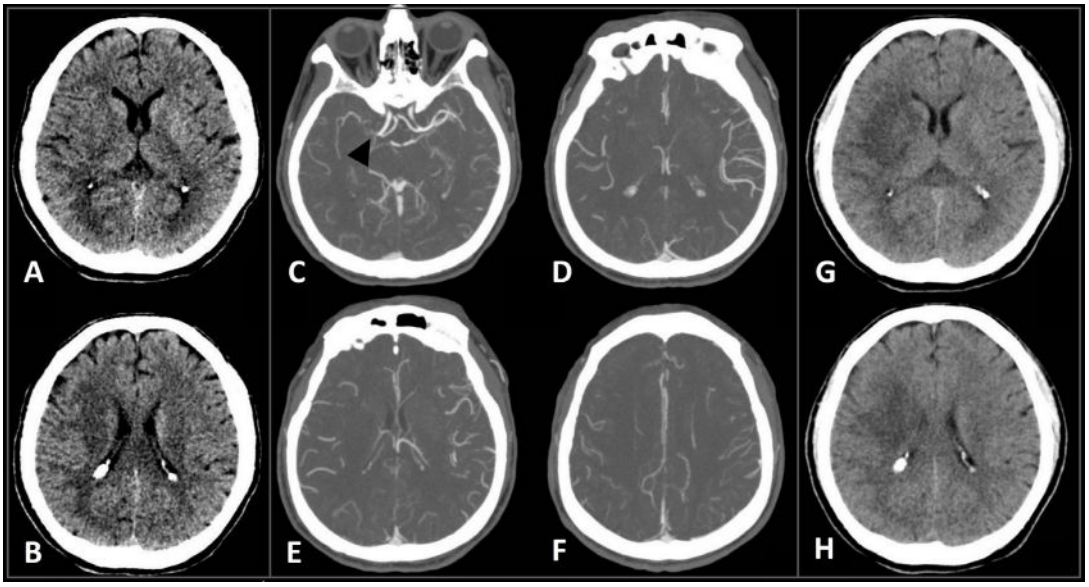

Figure 2. A *49-year-old male with acute right MCA infarction. Baseline NECT at 2 hours after onset (A and B) showed small hypodensity in posterior right insular cortex and right lentiform nucleus, ASPECTS = 8. Eight-mm axial MIP CTA (C-F) showed occlusion at right proximal M1 with good collaterals, score = 3; collateral filling =100% of the occlusion territory). Follow up NECT at 24 hours (G and H) showed small infarction in right insular lobe without hemorrhagic transformation.*

Discussion

Malignant MCA infarction is a serious complication of acute ischemic stroke involving large area of MCA territory. Life-threatening brain edema usually develops within thefirst few days after the stroke onset and may cause a midline shift and brain herniation. Clinical worsening and fatal outcome is up to 80% in conservative case [1,3,5]. Early decompressive craniectomy may help improve the functional outcome and reduce mortality. Imaging may help early predict this condition and facilitate prompt surgical management [3,6].

In these recent years, studies assessing collateral status in acute ischemic stroke emphasize on the impact on clinical outcome. Noninvasive CTA collateral score grading pial arterial filling of contrast media beyond the occluded site has been extensively used to evaluate the status of collateral circulation in patients with acute stroke. Data from IMS III trials and systematic review and meta-analysis revealed that in patients receiving endovascular treatment; robust collateral status was correlated with smaller infarct volume, reduced further infarct growth, reduced periprocedural symptomatic intracranial hemorrhage, better clinical outcome at 3 months, and could be used to select patients for endovascular treatment [10,21]. Recently, a systematic review and meta-analysis in the patients receiving intravenous thrombolysis alone without endovascular treatment also found that good pre-treatment collaterals were associated with smaller infarct size at baseline, a lower rate of symptomatic intracranial hemorrhage and a higher rate of early neurological improvement [22].

We have found that three studies focusing on assessment of clinical and imaging parameters, including CTA collateral status, to identify predictive factors of mMCAi. Kim et al[4] retrospectively reviewed 64 acute stroke patients with MCA occlusion within 8 hours after the symptom onset. Both patients receiving endovascular treatment and only intravenous thrombolysis were included. Recanalization of occluded arteries occurred in 21 patients. Clinical, laboratory and imaging parameters were analyzed for malignant brain edema. Baseline NIHSS >18 and CTA collateral score <2, using the same grading system as in our study, were found to be independent predictors of malignant brain edema.

Jo et al[19] retrospectively analyzed larger population of 121 patients with MCA occlusion. Recanalization of occluded arteries was achieved in 57 patients. They found 4 factors that were independently associated with malignant brain edema; which were baseline NIHSS, baseline NECT ASPECTS, CTA collateral status and revascularization failure. The same CTA grading system as our study was used again.

Flores et al[7] determined the impact of collateral circulation with development of mMACi, using multiphase CTA and The University of Calgary scoring system. Eighty-two patients with proximal MCA or ICA occlusion were prospectively included; 53 patients received endovascular treatment. Poor collateral circulation was found to be the only independent predictor of mMCAi.

In our study, we found a significant correlation between baseline NECT ASPECTS and CTA collateral status on development of mMCAi. After performing multivariate analysis, only baseline NECT ASPECTs was found to be an independent predictive factor for mMCAi. This discordant result may be due to the fact that we had a smaller number of patients and our patients may have lower baseline NECT ASPECTS compared to the mentioned studies.

We also found that patients with baseline ASPECTS ≤7 significantly were more likely to develop mMCAi compared to patients with ASPECTS >7. This result is in agreement with the study by MacCallum et al [23].

Multiphase CTA was developed by the University of Calgary and used in ESCAPE trial as one of the criteria of patient selection for endovascular treatment [17,18]. Multiphase CTA provides information on the degree and extent of pial arterial filling in a time resolved manner. Compared to multiphase CTA, single phase CTA potentially mislabel the delayed pial arterial filling and may underdiagnose the true collateral status [17]. However, a number of studies using single phase CTA for assessment of collateral status in stroke patients also showed a significant impact on the clinical outcome in both endovascular treatment and intravenous thrombolysis patient groups [21,22].

Our study has several potential limitations. First, our study is a retrospective study and may potentially have selection bias. Second, we did not have information about recanalization status that may affect the final infarct size. Finally, this study was performed at a single center and has a small sample size.

Conclusion

In patients with acute stroke with proximal MCA or ICA occlusion received only intravenous thrombolysis, baseline NECT ASPECTS and collateral status evaluated by single phase CTA showed significant correlation with development of malignant MCA infarction. However, only baseline NECT ASPECTS ≤ 7 was an independent predictor of malignant MCA infarction. CTA collateral status was not an independent predictive factor for this condition.

References

1. Hacke W, Schwab S, Horn M, Spranger M, De Georgia M, von Kummer R. 'Malignant' middle cerebral artery territory infarction: clinical course and prognostic signs. Arch Neurol 1996;53:309-15.

2. Ropper AH, Shafran B. Brain edema after stroke. Clinical syndrome and intracranial pressure. Arch Neurol 1984;41:26-9.

3. Heiss WD. Malignant MCA infarction: pathophysiology and imaging for early diagnosis and management decisions. Cerebrovasc Dis 2016;41:1-7. doi:10.1159/000441627.

4. Kim H, Jin ST, Kim YW, Kim SR, Park IS, Jo KW. Predictors of malignant brain edema in middle cerebral artery infarction observed on CT angiography. J Clin Neurosci 2015; 22:554–60.

5. Subramaniam S, Hill MD. Massive cerebral infarction. Neurologist 2005;11:150-60.

6. Staykov D, Gupta R. Hemicraniectomy in malignant middle cerebral artery infarction. Stroke 2011;42:513-6. doi: 10.1161/STROKEAHA.110.605642.

7. Flores A, Rubiera M, Ribó M, Pagola J, Rodriguez-Luna D, Muchada M, et al. Poor collateral circulation assessed by multiphase computed tomographic angiography predicts malignant middle cerebral artery evolution after reperfusion therapies. Stroke 2015;46:3149-53. doi:10.1161/STROKEAHA.115.010608.

8. Liebeskind DS. Collateral circulation. Stroke 2003;34:2279-84.

9. Nambiar V, Sohn SI, Almekhlafi MA, Chang HW, Mishra S, Qazi E, et al. CTA collateral status and response to recanalization in patients with acute ischemic stroke. AJNR Am J Neuroradiol 2014;35:884-90. doi: 10.3174/ajnr.A3817.

10. Menon BK, Qazi E, Nambiar V, Foster LD, Yeatts SD, Liebeskind D, et al. Differential effect of baseline computed tomographic angiography collaterals on clinical outcome in patients enrolled in the interventional management of stroke III trial. Stroke 2015;46:1239-44. doi: 10.1161/STROKEAHA.115.009009.

11. Christoforidis GA, Karakasis C, Mohammad Y, Caragine LP, Yang M, Slivka AP. Predictors of hemorrhage following intra-arterial thrombolysis for acute ischemic stroke: the role of pial collateral formation. AJNR Am J Neuroradiol 2009;30:165-70. doi: 10.3174/ajnr.A1276.

12. Bang OY, Saver JL, Kim SJ, Kim GM, Chung CS, Ovbiagele B, et al. Collateral flow predicts response to endovascular therapy for acute ischemic stroke. Stroke 2011;42:693-9. doi: 10.1161/STROKEAHA.110.595256.

13. Liebeskind DS, Tomsick TA, Foster LD, Yeatts SD, Carrozzella J, Demchuk AM, et al. Collaterals at angiography and outcomes in the Interventional Management of Stroke (IMS) III trial. Stroke 2014;45:759-64. doi: 10.1161/STROKEAHA.113.004072.

14. Yeo LL, Paliwal P, Low AF, Tay EL, Gopinathan A, Nadarajah M, et al. How temporal evolution of intracranial collaterals in acute stroke affects clinical outcomes. Neurology 2016;86:434-41. doi:10.1212/WNL.0000000000002331.

15. Fanou EM, Knight J, Aviv RI, Hojjat SP, Symons SP, Zhang L, et al. Effect of collaterals on clinical presentation, baseline imaging, complications, and outcome in acute stroke. AJNR Am J Neuroradiol 2015;36:2285-91. doi: 10.3174/ajnr.A4453.

16. Brunner F, Tomandl B, Hanken K, Hildebrandt H, Kastrup A. Impact of collateral circulation on early outcome and risk of hemorrhagic complications after systemic thrombolysis. Int J Stroke. 2014;9:992-8. doi: 10.1111/j.1747-4949.2012.00922.x.

17. Menon BK, d'Esterre CD, Qazi EM, Almekhlafi M, Hahn L, Demchuk AM, et al. Multiphase CT angiography: a new tool for the Imaging triage of pa tients with acute ischemic stroke. Radiology 2015;275:510-20. doi: 10.1148/radiol.15142256.

18. Goyal M, Demchuk AM, Menon BK, Eesa M, Rempel JL, Thornton J, et al. Randomized assessment of rapid endovascular treatment of ischemic stroke. N Engl J Med 2015 ; 372:1019-30. doi: 10.1056/NEJMoa1414905.

19. Jo K, Bajgur SS, Kim H, Choi HA, Huh PW, Lee K. A simple prediction score system for malignant brain edema progression in large hemispheric infarction. PLoS One 2017; 12(2):e0171425. doi: 10.1371/journal.pone.0171425. eCollection 2017.

20. Berger C, Fiorelli M, Steiner T, Schäbitz WR, Bozzao L, Bluhmki E, et al. Hemorrhagic transformation of ischemic brain tissue: asymptomatic or symptomatic? Stroke 2001; 32:1330-5.

21. Leng X, Fang H, Leung TW, Mao C, Miao Z, Liu L, et al. Impact of collaterals on the efficacy and safety of endovascular treatment in acute ischaemic stroke: a systematic review and meta-analysis. J Neurol Neurosurg Psychiatry 2016;87:537-44. doi: 10.1136/jnnp-2015-310965.

22. Leng X, Lan L, Liu L, Leung TW, Wong KS. Good collateral circulation predicts favorable outcomes in intravenous thrombolysis: a systematic review and meta-analysis. Eur J Neurol 2016;23:1738-49. doi: 10.1111/ene.13111.

23. MacCallum C, Churilov L, Mitchell P, Dowling R, Yan B. Low Alberta Stroke Program Early CT score (ASPECTS) associated with malignant middle cerebral artery infarction. Cerebrovasc Dis 2014;38:39-45. doi:10.1159/000363619.

Case Report

Hepatic hemangioma in cirrhosis : Two case reports

Kinley S Dorji, M.D.
Sunpob Cheewadhanaraks, M.D.
From Department of Radiology, Faculty of Medicine, Prince of Songkla University, Songkhla, Thailand.
Address correspondence to K.D. (e-mail: kinleykai23@yahoo.com)

Abstract

Hepatic hemangioma is the most common primary liver tumor with the reported prevalence of 0.4-20%. However, the prevalence of hepatic hemangioma in cirrhosis is considered to be very low ranging from 1.2-1.7%. Also, the morphology and hemodynamics of the hemangioma are different from those found in a non-cirrhotic liver. We reported two cases of hepatic of hemangioma in cirrhosis and their natural progression on a follow-up

Keywords: Hepatic hemangioma, Cirrhosis, Progression.

Introduction

Hepatic hemangioma is the most common primary liver tumor with the prevalence of 0.4-20%[1–3]. It is a benign tumor composed of vascular spaces lined by endothelial cells. In contrast, the prevalence of hepatic hemangioma in cirrhotic patients is considered to be very low ranging from 1.2-1.7 %[4, 5]. Cirrhosis is the end stage of the chronic liver injury characterized by the development of regenerative nodules and surrounding fibrosis. In addition to lower prevalence, the morphology and hemodynamics of hemangioma are different from those found in a non-cirrhotic liver. This is believed to be a result of alteration of blood flow and intra-hepatic environment due to fibrosis in cirrhosis. We reported two cases of hepatic hemangioma in cirrhotic liver and their natural progression.

Case Summary

Case 1

A 56-year-old woman, who is a known case of hypertension and chronic hepatitis C on interferon and ribavirin for 24 weeks, presented with relapse (high viral load) despite good compliance. She was asymptomatic. Her blood pressure was under control and physical examinations were unremarkable. The laboratory result showed mildly elevated liver enzymes. The initial ultrasound scan(USS) showed early features of cirrhosis with an ill-defined hyperechoic nodule in segment VII which could have been either hemangioma or hepatocellular carcinoma(HCC) (Figure 1).

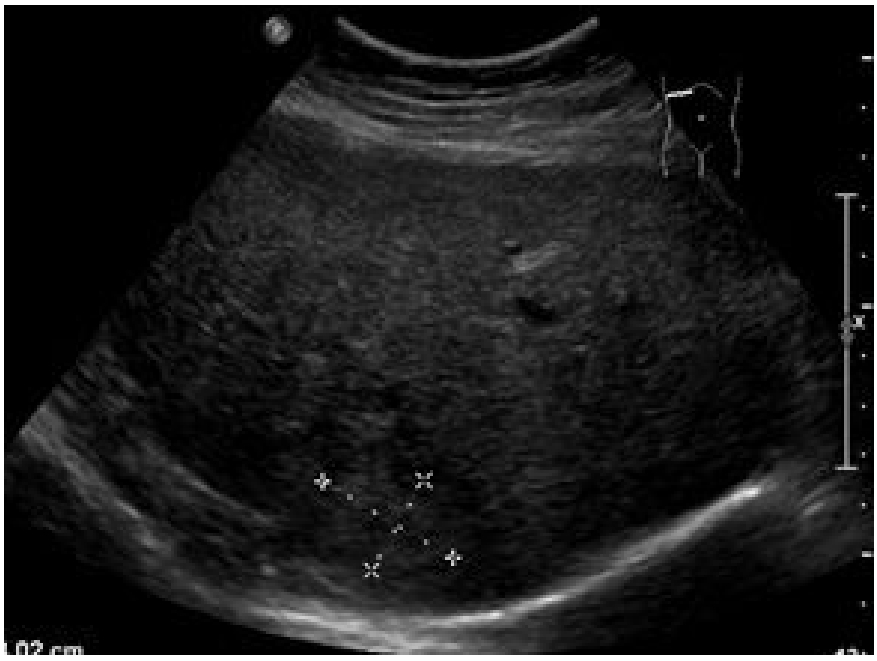

Figure 1: *USS showing ill-defined hyperechoic nodule (marked) in hepatic segment VII.*

Therefore, computed tomography (CT) and magnetic resonance imaging (MRI) of the abdomen were performed which confirmed the diagnosis of hemangioma at segment VII (Figure 2 and 3). No HCC was discovered.

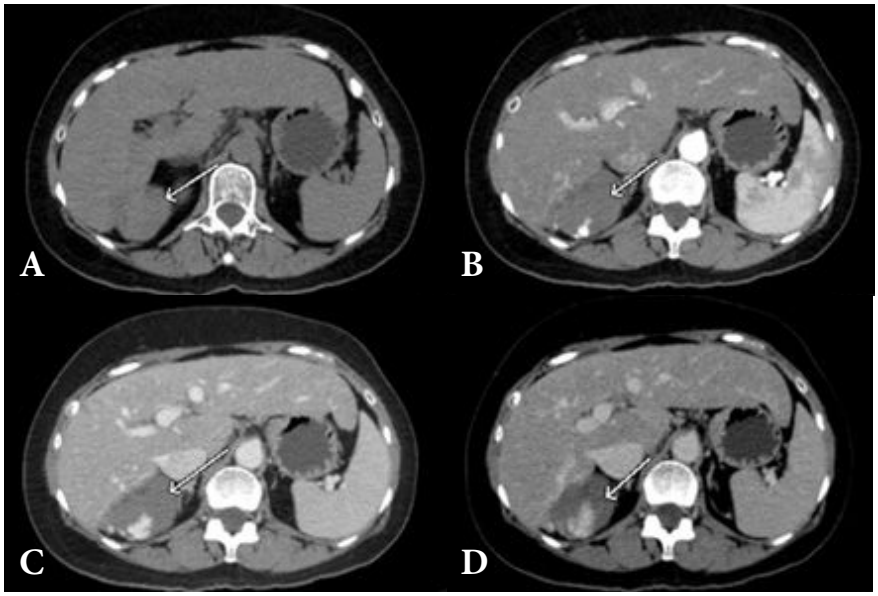

Figure 2: *CT upper abdomen in A) plain, B) arterial, C) venous and D) delayed phase showing cirrhotic liver with lobulated hypodense mass and peripheral nodular progressive enhancement typical for hemangioma (arrow) in segment VII. Two small hypodense lesions with homogenous enhancement pattern matching blood pool(flash-filling) was seen at segment II and III, typical of small hemangioma (not shown).*

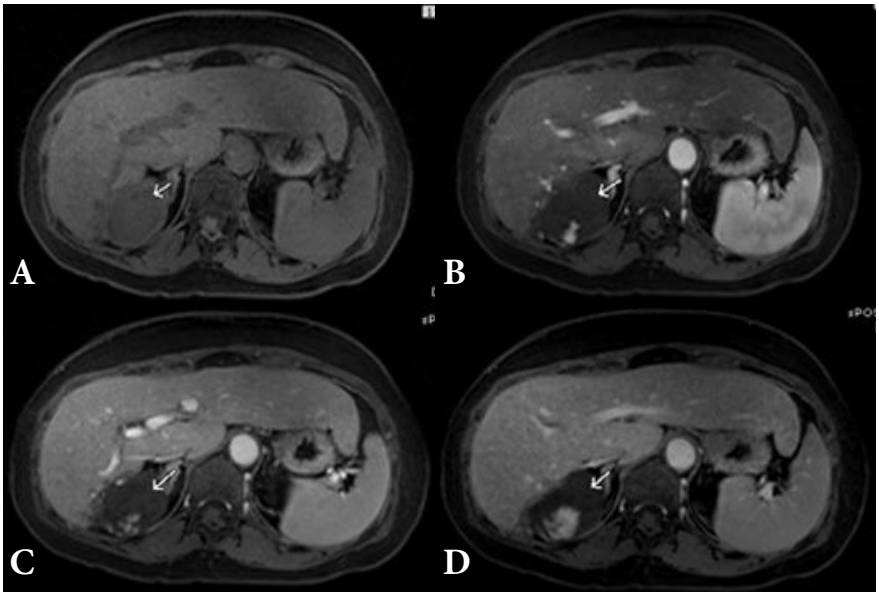

Figure 3: *MRI upper abdomen A) pre-gadolinium B) 30 seconds(s), C) 60s and D) 120s showing early features of cirrhosis with typical enhancing pattern of hemangioma (arrow) in segment VII.*

She was restarted interferon and ribavirin which was continued for 43 weeks without any complications. At the end of an anti-viral therapy, rapid and sustained virological response was achieved. She continued to undergo a routine USS liver with occasional MRI/CT scan. The follow-up images showed progressive cirrhosis of the liver with decreased size of hepatic hemangioma in segment VII while the hemangioma at segments II and III disappeared. On top of that, the peripheral nodular and progressive centripetal enhancement was not observed. Instead, irregular progressive enhancement seen in only some parts of the hemangioma was noted and the lesion was diagnosed as atypical hemangioma. Eventually, the hemangioma became avascular.

Later on, the patient developed small HCC, about 1.0 cm, in segment IVA/VIII, about 7 years later which was treated successfully with two sessions of selective transarterial chemoembolization (sTACE) (Figure 4).

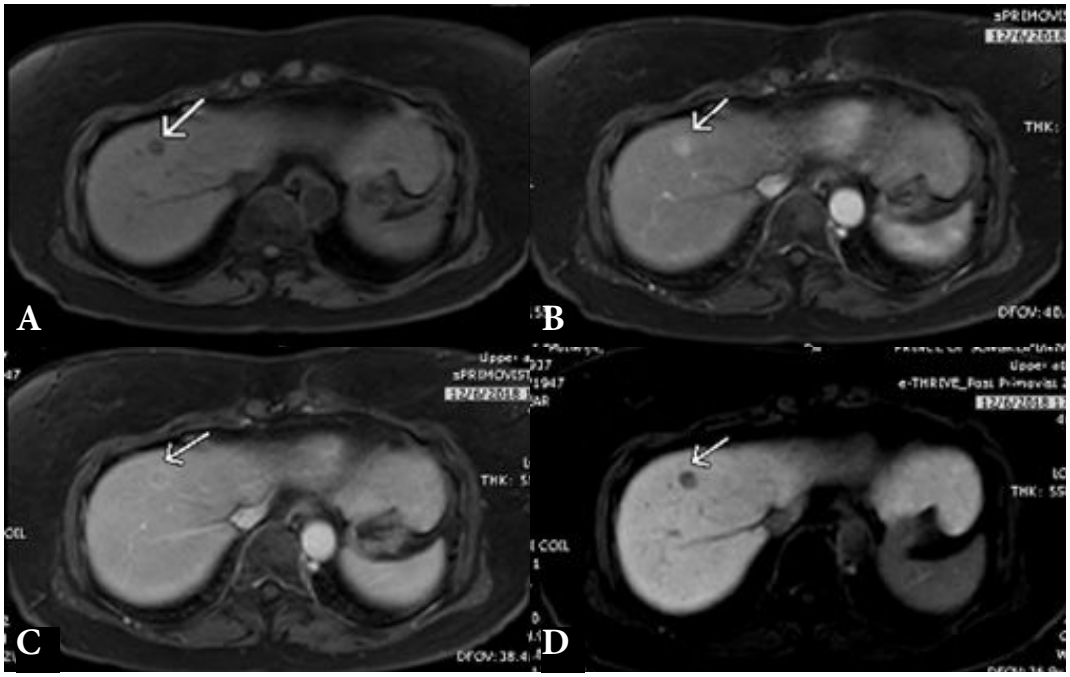

Figure 4: *MRI liver A) pre-gadolinium, B) 30s, C) 60s and D) primovist 20 minutes showing a small nodule (arrow) in segment 4A/8 with early arterial hyperenhacement, rapid venous washout and no primovist uptake at 20 minutes, highly suggestive of HCC.*

The latest MRI scan showed previously seen hemangioma as a T2 hyperintense lesion at segment VII without enhancement (avascular). No recurrent or new HCC was noted (Figure 5).

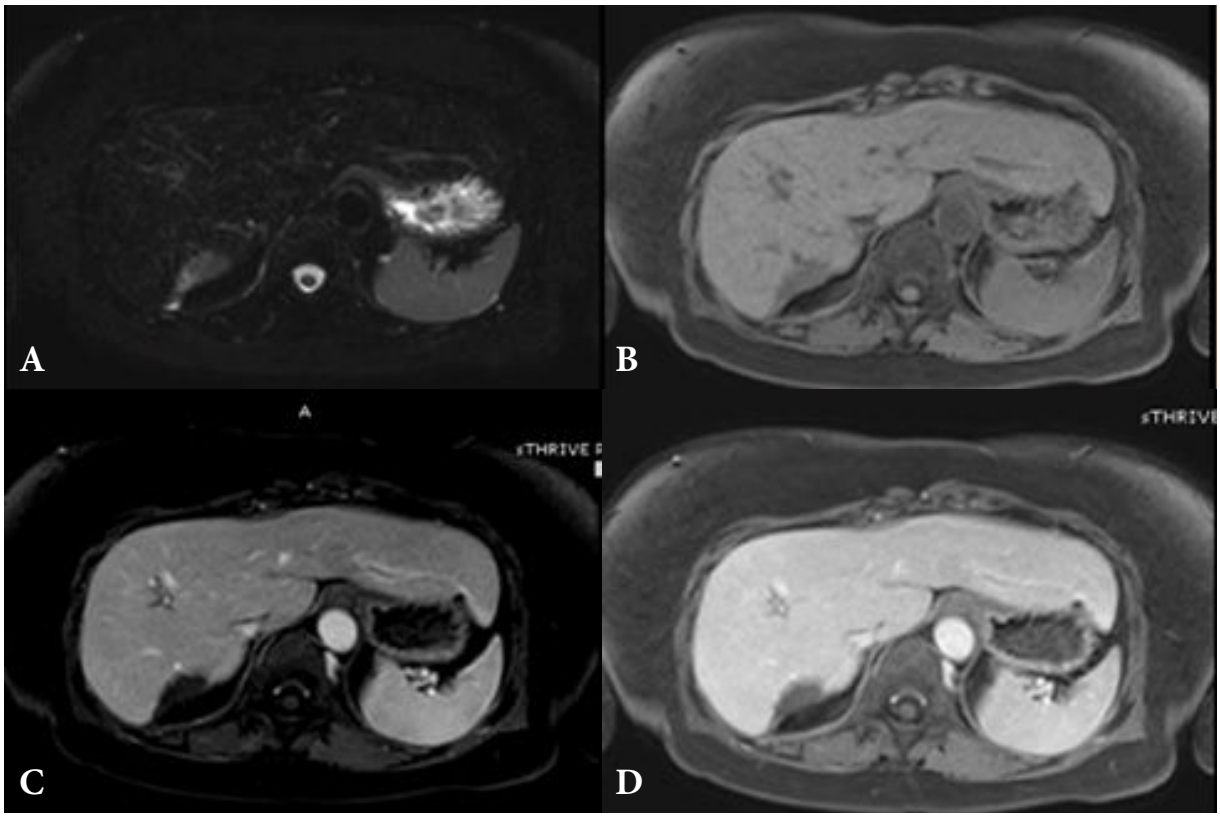

Figure 5: *MRI liver A) T2*, B) pre-gadolinium, C) 60s and D) 120s showing avascular T2 hypersignal lesion in segment VII with progressive cirrhosis.*

Case 2

A 52-year-old female, who is a known case of chronic hepatitis C with cirrhosis and portal hypertension, presented with a well-defined heterogeneous mass and a few small hyperechoic nodules at segment VII during routine HCC surveillance on the ultrasound scan which was likely to be hemangioma (Figure 6).

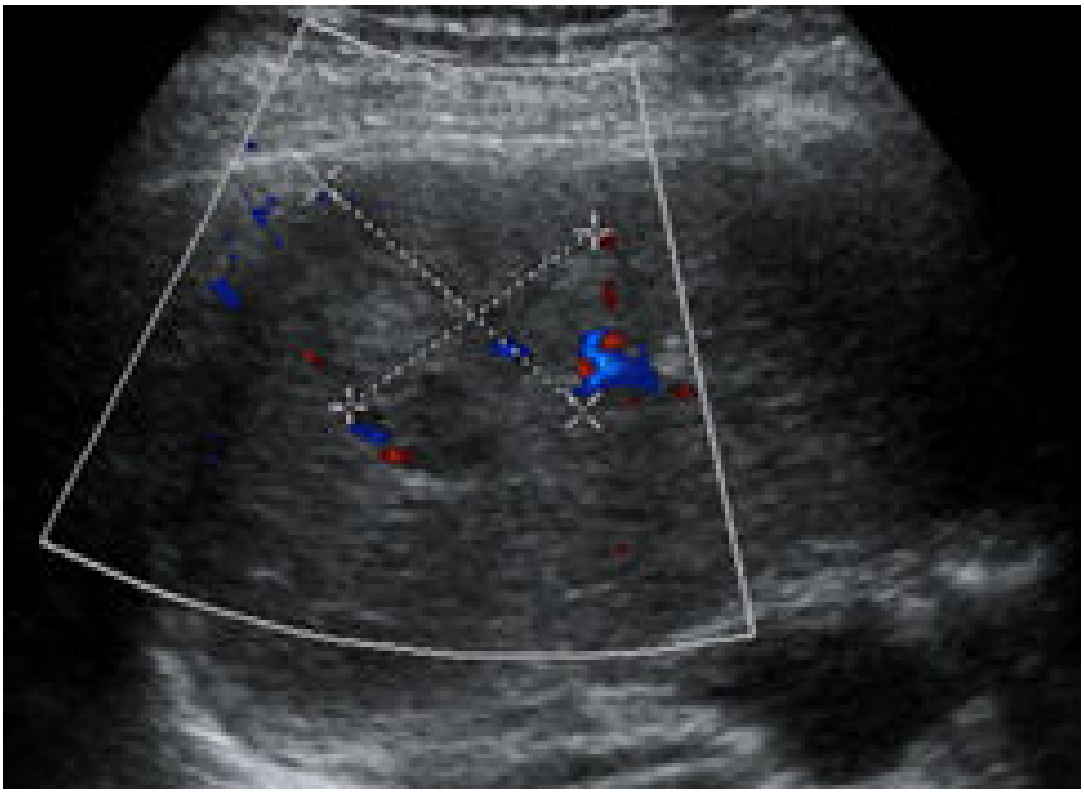

Figure 6: *USS liver showing well-defined heterogeneous hyperechoic mass (marked) with internal hypoechogenicity and internal flow at segment VII, likely to be hemangioma. Small hyperechoic nodules were also seen, likely to be small hemangiomas (not shown).*

Further evaluation and imaging were advised. The contrast-enhanced CT and MRI liver showed cirrhotic liver with a well-defined hypodense subcapsular mass with peripheral nodular and progressive centripetal enhancement, completely filling in, in segment VII, typical of hemangioma (Figure 7 and 8). No HCC was noted.

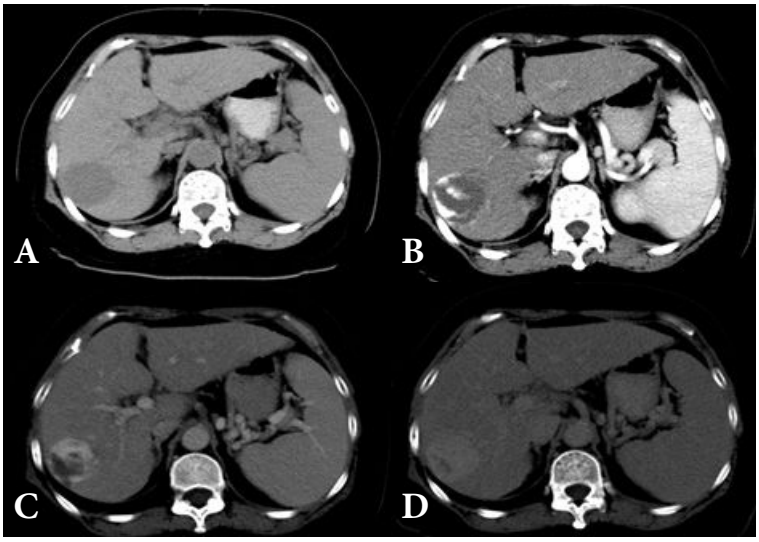

Figure 7: *CT liver A) plain, B) arterial, C) venous and D) delayed phase showing peripheral nodular with progressive centripetal enhancement at segment VII, characteristic of hemangioma.*

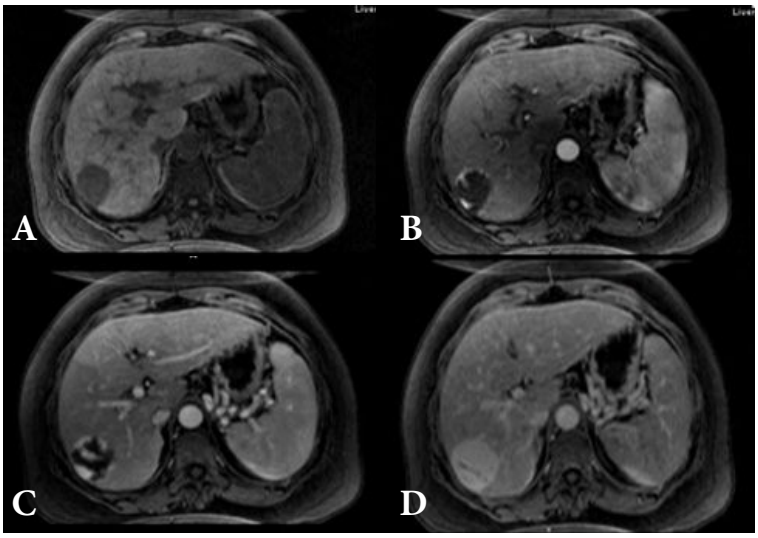

Figure 8: *MRI liver A) plain, B) 30s, C) 60s and D) 120s showing peripheral nodular with progressive centripetal enhancement at segment VII, characteristic of hemangioma.*

The most recent contrast enhanced CT abdomen scan showed a decrease in the size of previously seen hemangioma at segment VII with less intense and atypical enhancement pattern (Figure 9).

Figure 9: *CT abdomen A) plain, B) arterial and C) venous phase showing decrease size of previously seen hemangioma (arrow) at segment VII. A less obvious typical enhancing pattern of hemangioma with enhancement seen only in some parts of the lesion.*

Discussion

Hemangioma is the most common primary tumor of the liver. It has the prevalence of 0.4-20% [1–3]. It is a benign tumor consisting of vascular spaces lined by endothelial cells. The exact etiology or pathophysiology of hemangioma is not known. However, they are thought to be congenital vascular malformation or hamartoma. It is most commonly found in adults between 30-50 years old and is more common among females with a 3:1 ratio [6]. Most hemangioma are asymptomatic and are diagnosed incidentally when investigated for other pathologies. However, some hemangioma especially giant hemangioma(>10 cm), can present with symptoms such as right upper quadrant pain, discomfort, early satiety, nausea and vomiting [7]. No malignant transformation of hemangioma has been reported so far[8].

Cirrhosis is the end stage of the chronic liver injury characterized by the development of regenerative nodules and surrounding fibrous bands. According to the Global Burden of Disease (GBD), Thailand has the highest incidence of cirrhosis in Asia[9]. The common causes of cirrhosis in Asia include chronic viral hepatitis (B and C)[10]. Other causes of cirrhosis include alcoholic liver disease, non-fatty liver disease, hemochromatosis, autoimmune, cystic fibrosis and so on. In both of our cases, the patient had been diagnosed with chronic hepatitis C infection and they developed cirrhosis.

Unlike the general hepatic hemangioma prevalence, the prevalence of hemangioma in the cirrhotic liver is considered to be very low ranging from 1.2-1.7 %[4, 5]. However, these data were older than two decades ago which was based exclusively on histopathological findings (autopsies and surgical specimens). According to the more recent study, the prevalence of the hepatic hemangioma in cirrhosis was 8.8% and there was no statistically significant difference with the prevalence in the non-cirrhotic liver[11]. Now with the advancement in both technologies, protocols, better understanding of the histopathology as well as the increasing amont of imaging (CT/MRI), the prevalence of hemangioma is expected to be much higher than previously reported.

Many believe that as the cirrhosis progresses, it alters the morphology and hemodynamics of the hemangioma[12]. The previous studies have shown that the hemangioma in cirrhosis tends to be smaller in size which could be attributable to obliteration from fibrosis seen in cirrhosis[13–15]. One case in a study even reported a complete disappearance of hemangioma in cirrhosis[14]. Dodd et al demonstrated extensive fibrosis within and surrounding hemangioma in cirrhotic liver specimens[4]. The decreased blood flow in cirrhosis is thought to alter hemodynamics of the hemangioma. Typically, the hemangioma will appear as well-defined hypodense or pre-gadolinium hypointense in the unenhanced image and after contrast injection; it will show characteristic peripheral nodular and progressive centripetal enhancement, matching with the blood pool all the time[7]. Additionally, in T2 and T2* MRI sequence, the hemangioma will appear

bright and 'light-bulb' bright respectively. However, in case of small hemangiomas (<2 cm), they might show homogenous enhancement described as flash-filling while giant hemangioma might show incomplete central filling in. All these characteristic enhancing patterns of hemangioma are either lost or not obvious in cirrhosis[16]. In both of our cases, they presented with a well-defined subcapsular lesion in segment VII showing peripheral nodular and progressive centripetal enhancement typical of hemangioma. The hemangioma in both patients was hyperintense in T2 and light bulb bright in T2*. No active biopsy or intervention was done as the imaging features were characteristic of hemangioma.

During the follow-up in both cases, the hemangioma gradually decreased in size. The intensity of the enhancement also decreased with rather incomplete centripetal filling in. In the first case, the hemangioma eventually became avascular without any enhancement while in the second case, minimal enhancement was observed in some parts of the lesion. No hemangioma associated capsular retraction was seen which is in agreement with Soyer et al which stated that capsular retraction adjacent to the hepatic tumor is a specific sign of hepatic neoplasm [17].

HCC is the fifth commonest cause of cancer and the second commonest of cancer-related deaths in the world[18]. Cirrhosis is a known risk factor for HCC with >90% HCC developing in the cirrhotic liver[19]. The risk of HCC in HCV-infected patients is increased by 15- to 20-fold, with an annual incidence of HCC being estimated at 1-4% in cirrhotic over a 30-year period[20]. The first case eventually developed HCC at segment 4A/8 and was treated successfully with two sessions of sTACE.

Conclusion

The prevalence of the hepatic hemangioma in the cirrhotic liver might be higher than previously estimated. The cirrhosis alters the morphology and hemodynamics of hepatic hemangioma resulting in a decreased size and loss of the characteristic enhancement pattern.

References

1. European Association for the Study of the Liver (EASL). EASL Clinical Practice Guidelines on the management of benign liver tumours. J Hepatol 2016; 65: 386–98.

2. Rungsinaporn K, Phaisakamas T. Frequency of abnormalities detected by upper abdominal ultrasound. J Med Assoc Thai 2008; 91: 1072–75.

3. Bahirwani R, Reddy KR. Review article: the evaluation of solitary liver masses. Aliment Pharmacol Ther 2008; 28: 953–65.

4. Dodd GD 3rd, Baron RL, Oliver JH 3rd, Federle MP. Spectrum of imaging findings of the liver in end-stage cirrhosis: Part II, focal abnormalities. AJR Am J Roentgenol 1999;173:1185-92.

5. Karhunen PJ. Benign hepatic tumours and tumour like conditions in men. J Clin Pathol 1986; 39: 183–88.

6. Gandolfi L, Leo P, Solmi L, Vitelli E, Verros G, Colecchia A. Natural history of hepatic haemangiomas: clinical and ultrasound study. Gut 1991; 32: 677–80.

7. Bajenaru N, Balaban V, Săvulescu F, Campeanu I, Patrascu T. Hepatic hemangioma -review-. J Med Life 2015; 8 Spec Issue: 4-11.

8. Flucke U, Vogels RJ, de Saint Aubain Somerhausen N, Creytens DH, Riedl RG, van Gorp JM, et al. Epithelioid Hemangioendothelioma: clinicopathologic, immunhistochemical, and molecular genetic analysis of 39 cases. Diagn Pathol 2014 ; 9: 131.

9. Byass P. The global burden of liver disease: a challenge for methods and for public health. BMC Med 2014; 12: 159.

10. Wong MCS, Huang J. The growing burden of liver cirrhosis: implications for preventive measures. Hepatol Int 2018; 12: 201-3.

11. Galvão BVT, Torres LR, Cardia PP, Nunes TF, Salvadori PS, D'lppolito G. Prevalence of simple liver cysts and hemangiomas in cirrhotic and non-cirrhotic patients submitted to magnetic resonance imaging. Radiol Bras 2013; 46: 203-8.

12. Bartolozzi C, Cioni D, Donati F, Lencioni R. Focal liver lesions: MR imaging-pathologic correlation. Eur Radiol 2001; 11: 1374–388.

13. Yamashita Y, Ogata I, Urata J, Takahashi M. Cavernous hemangioma of the liver: pathologic correlation with dynamic CT findings. Radiology 1997; 203: 121–5.

14. Mastropasqua M, Kanematsu M, Leonardou P, Braga L, Woosley JT, Semelka RC. Cavernous hemangiomas in patients with chronic liver disease: MR imaging findings. Magn Reson Imaging 2004; 22: 15–8.

15. Yu JS, Kim KW, Park MS, Yoon SW. Hepatic cavernous hemangioma in cirrhotic liver: imaging findings. Korean J Radiol 2000; 1: 185–90.

16. Brancatelli G, Federle MP, Blachar A, Grazioli L. Hemangioma in the Cirrhotic Liver: Diagnosis and Natural History. Radiology 2001; 219: 69–74.

17. Soyer P. Segmental anatomy of the liver: utility of a nomenclature accepted worldwide. AJR Am J Roentgenol 1993; 161: 572–3.

18. Bosetti C, Turati F, La Vecchia C. Hepatocellular carcinoma epidemiology. Best Pract Res Clin Gastroenterol 2014; 28: 753–70.

19. Flemming JA, Yang JD, Vittinghoff E, Klm WR, Terrault NA. Risk Prediction of Hepatocellular Carcinoma in Patients With Cirrhosis: The ADRESS-HCC Risk Model. Cancer 2014; 120: 3485–93.

20. El-Serag HB. Epidemiology of viral hepatitis and hepatocellular carcinoma. Gastroenterology 2012; 142: 1264-1273.e1.

Case Report

Multiple pulmonary nodules mimicking metastasis in a case of systemic amyloidosis

Kaewkamol Srichai, M.D.[(1)]
Warath Chantaksinopas, M.D.[(1)]
Papon Prettiwitayakul, M.D.[(1)]
Kanet Kanjanapradit, M.D.[(2)]
From [(1)] Department of Radiology, Faculty of Medicine, Prince of Songkla University, Songkhla, Thailand.
[(2)]Department of Pathology, Faculty of Medicine, Prince of Songkla University, Songkhla, Thailand.
Address correspondence to K.S. (e-mail: drkaew021@gmail.com)

Abstract

Amyloidosis is a disorder resulting from the abnormal accumulation of amyloid, a fibrillary protein, in various tissues and organs. Pulmonary amyloidosis can be a part of a systemic process and can mimic other lung diseases which present with multiple pulmonary masses or nodules, such as metastasis.

We reported a case of systemic amyloidosis, which is histopathologically confirmed from the nasal lesion, initially presented with multiple lung nodules mimicking pulmonary metastasis but had been stable for years. Pathological study of tissues obtained from three times of percutaneous transthoracic needle biopsy (PTNB) failed to show specific features. The findings on chest radiographs, contrast enhanced thoracic computed tomography (CT) and histology were reviewed and discussed.

Keywords: Amyloidosis, Pulmonary amyloidosis, Systemic amyloidosis, Chest CT, Pulmonary metastasis.

Introduction

Amyloidosis is an uncommon systemic disorder that is characterized by extracellular accumulation and deposition of abnormal protein and protein derivatives [1, 2]. No clear genetic or environmental factors in individual susceptibility to amyloid deposition have been made [3]. Amyloidosis can be systemic or localized. Systemic amyloidosis is subclassified into a primary (idiopathic) form and a secondary (reactive) form. Tuberculosis, familial Mediterranean fever, rheumatoid arthritis, or multiple myeloma are the causes of secondary amyloidosis [4]. The disease becomes clinically significant when its diffuse form affects organ function by replacing the normal cell structure [1]. The most commonly involved organs in patients with systemic amyloidosis are the heart and kidneys, followed by the nervous system, soft tissue, lungs, and liver. The involvement of the lungs is relatively common but rarely symptomatic. The most common symptoms of amyloid involvement with the respiratory system are coughs, wheezing, dyspnea on exertion, and hemoptysis [4, 5].

Case summary

A 61-year-old Thai female presented with abdominal discomfort for 2 months with mild pelvic pain, loss of appetite, constipation, and insignificant low-grade fever. No gynecologic symptoms were recorded. Her underlying disease included hypertension and GERD. She also underwent left salphingo-oophorectomy due to benign condition. Her physical examination revealed no fever and unremarkable vital signs. The abdominal and gynecologic examinations showed a low midline surgical scar without abnormal mass. Small-sized cervix, and normal uterus were noted. Her laboratory result revealed a low hemoglobin level (10.7 g/dL) but a normal white cell count and platelets. The liver and renal functions as well as urinalysis were unremarkable. The routine chest radiograph showed multiple lung nodules which were varying in size (Figure 1). The contrast enhanced abdominal CT scan showed an ill-defined heterogeneous mass at the anterior aspect of the uterus (Figure 2). The contrast enhanced chest CT scan revealed multiple enhanced spiculated and well-defined nodules scattered in both lungs (Figure 3). Her diagnosis was the pelvic mass with lung metastasis, suspicious of uterine sarcoma.

Figure 1: *The frontal chest radiograph shows a well-defined nodule in the right lower lung field. A few smaller nodules in both upper lobes are also detected.*

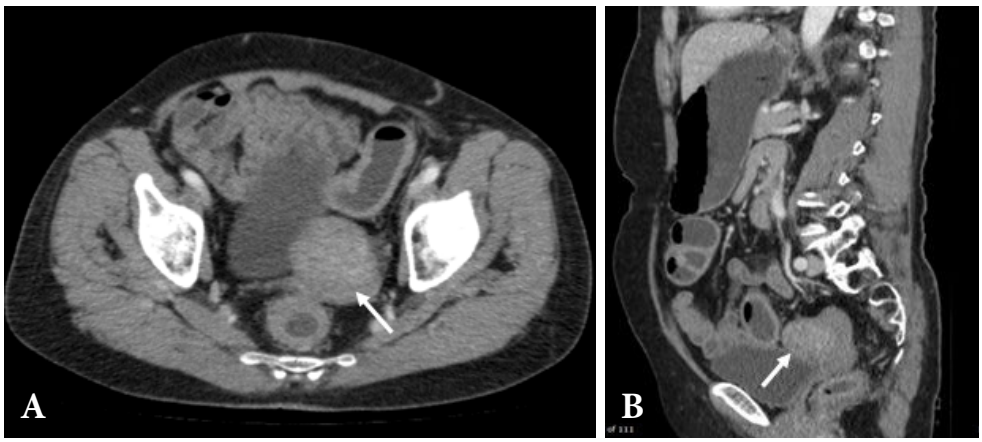

Figure 2: *Contrast enhanced abdominal CT scan in axial (A) and reformatted sagittal (B) images show an ill-defined homogeneous mass at anterior aspect of the uterine fundus (arrow).*

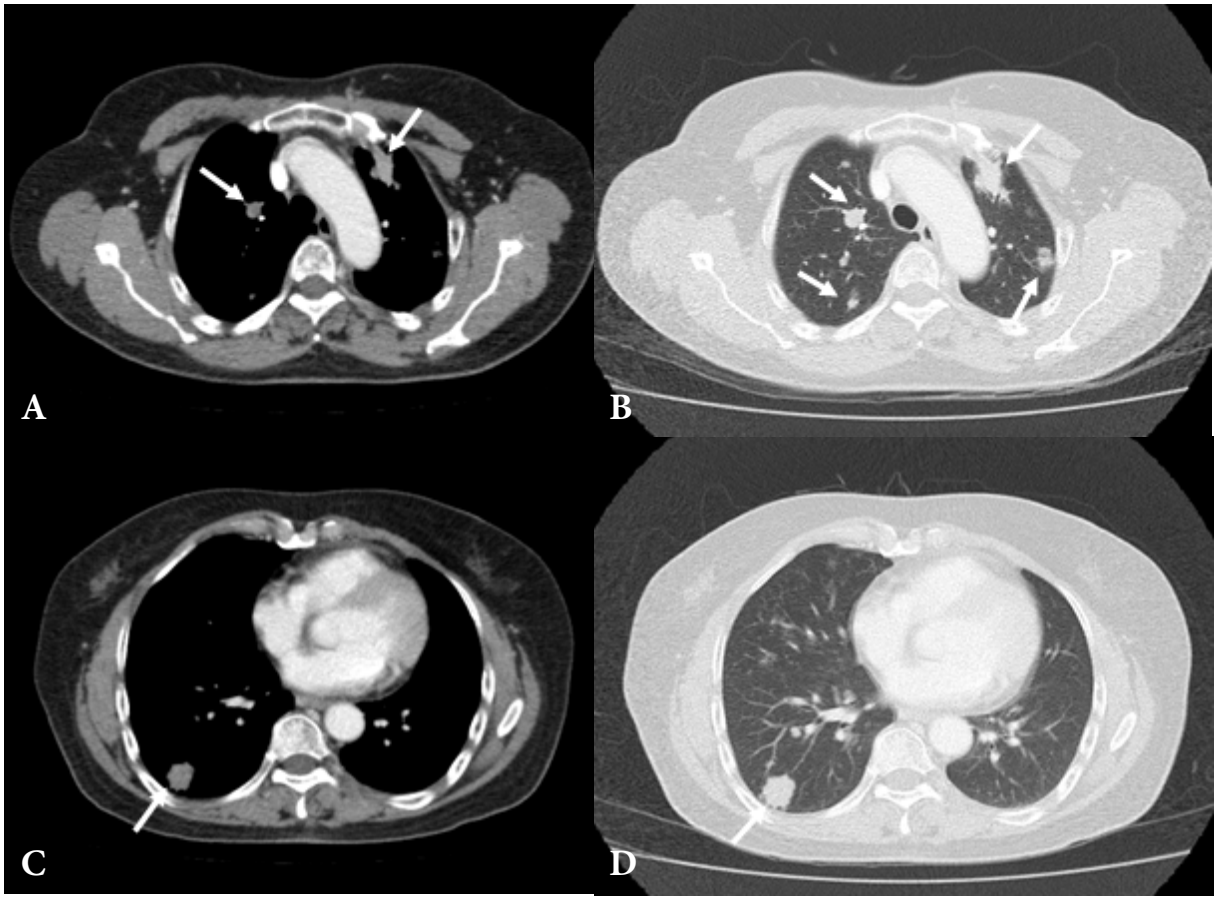

Figure 3: *Contrast enhanced chest CT scan in mediastinal and lung windows at the level of aortic arch (A, B) and at the level of inferior pulmonary veins (C, D) show multiple heterogeneously enhanced spiculated and well-defined nodules scattered in both lungs which has no zonal predominance (arrow). These nodules are vary in size. No internal calcification or necrotic portion is observed.*

The patient underwent transvaginal ultrasonography which revealed 6.6x4.3 cm uterus with a small subserous myoma at the posterior wall and thin endometrium. Both ovaries were not visualized. Because of benign ultrasonographic appearance, the gynecologist suggested tissue diagnosis from the lung instead of the uterus.

Percutaneous transthoracic needle biopsy (PTNB) was done at the largest lesion in the right lower lobe but the pathological result reported only small fragments of benign tissue; therefore, repeat biopsy was suggested. However, the patient lost follow-up.

Nearly two years later, the patient revisited our hospital, without any abnormal symptoms. She was transferred to the gynecologic department. Endometrial biopsy was done but the tissue was not sufficient for diagnosis while the Papanicolaou test showed a negative result for malignancy. The chest CT scans were done to re-evaluate disease progression, which showed rather stable nodules in both lungs. The second PTNB was done. The result was positive for glycoprotein material; periodic acid-Schiff (PAS)-positive, PAS with predigestion with diastase (PASD)-non-reactive, Congo red-negative; therefore, pathologist suspected pulmonary alveolar proteinosis (PAP). The patient was then referred to the chest unit.

After reviewed of all images, the PTNB was done for the third time to determine pulmonary metastasis, while the lesion at the uterus might be an asymptomatic myoma uteri due to its stable nature. The third PTNB showed a small fragment of benign lung tissue with chronic inflammation and tissue necrosis without a definite area of carcinoma. The pathological diagnosis was pulmonary alveolar proteinosis.

A year later, the patient developed left-sided nasal swelling. The physical examination revealed left lateral nasal ala swelling, hard consistency, and irregular skin tag. Because the symptom persisted after she received adequate topical medical treatment, a biopsy was performed. The specimen showed the deposition of eosinophilic amorphous material in the submucosal tissue with the displaced capillary lumen. The additional Congo red stain of the specimen showed apple-green birefringence under the polarized microscope (Figure 4). Therefore, the pathologic findings were compatible with amyloidosis. The chest unit was notified, and the possibility of systemic amyloidosis was discussed.

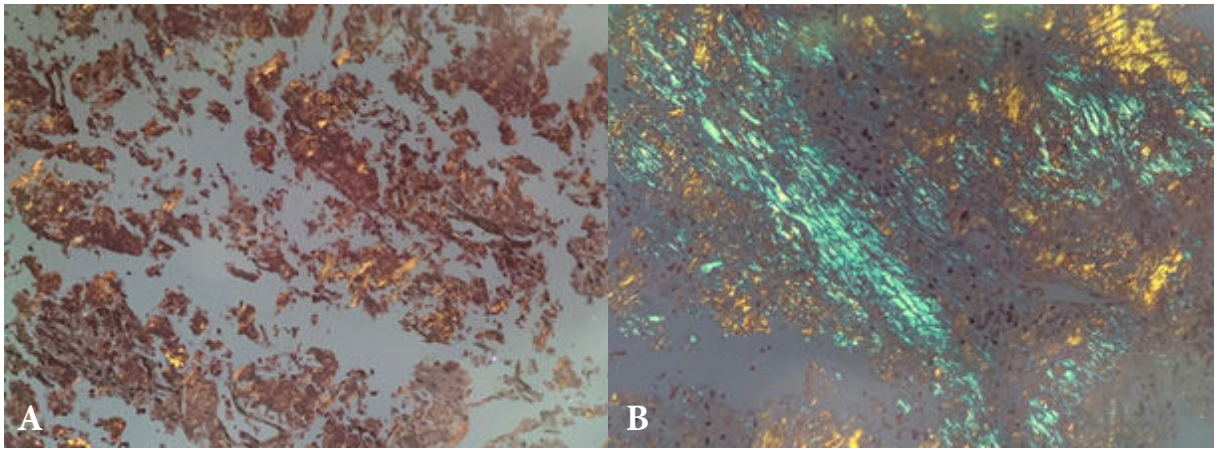

Figure 4: *Specimen from the left nasal alar surgical biopsy with Congo red staining (A) shows the deposition of eosinophilic amorphous material in the submucosal tissue which also shows apple-green birefringence under the polarized microscope (B).*

Diagnosis :

1. Systemic amyloidosis with nasal and pulmonary involvement.
2. Asymptomatic myoma uteri

Discussion

Three different forms of amyloidosis in the lungs from the pathologist's perspective include nodular pulmonary amyloidosis, diffuse alveolar-septal amyloidosis and tracheobronchial amyloidosis [5]. In Zhang et al[6] study, there is no specific clinical findings, examination, laboratory tests and radiological results for the diagnosis of nodular parenchymal pulmonary amyloidosis. The specimen with amyloid deposit shows apple-green birefringence when stained with Congo red and viewed under polarized light [1,6].

In our study, the pulmonary findings revealed multiple nodules in both lungs which were stable after a follow-up on CT scan and CXR. During metastatic work up, the patient developed hard consistency irregular skin tag at the left lateral nasal alar. The final histopathological report was consistent with amyloidosis. Although

the pathological result from the second PTNB was suspected of PAP but both PAP and amyloid disease may have common disturbances in immunoregulatory mechanisms as an important step in the pathogenesis [7]. In conclusion, pulmonary nodular amyloidosis was considered in this case, mimicking primary pulmonary or metastatic neoplasms.

In the previous studies, multiple deposits are commonly found in nodular parenchymal amyloid rather than focal deposits. Calcification is seen in about 50% of the cases, often centrally or in an irregular pattern within the nodule. The nodules may be of multiple shapes, sizes varying from 0.5 to 15 cm and with slow growth, often over years, and no regression [4]. CT can suggest the diagnosis because it is a good tool to demonstrate subtle calcification, which is often found in amyloidosis. The typical locations are peripherally or subpleural. Cavitation is very rare [4].

The hyperdensity of the multiple pulmonary nodules compared to muscle in our case, showed no clear explanation. They could be parts of calcification which is an important characteristic that can be found in almost half of the cases or increased enhancement which is suspected from morphologic alterations from amyloid deposition [4, 11]. However, the histopathological report revealed no calcification or structural alteration, such as neovascularization or granulation tissue, that can elucidate increased contrast enhancement. Eventually, the lesions could be hyperattenuated on unenhanced CT, which are observed in the brain [12]. However, no plain CT in our study was performed.

The cases reported by Zhang et al [6] and Seo et al [8], exhibited multiple lung nodules of pulmonary amyloidosis with moderate 18F-FDG uptake. Positive results of 18F-FDG PET/CT on pulmonary nodules should be interpreted with caution in differentiating pulmonary nodular amyloidosis from malignant lesions. Histological confirmation is required for the final diagnosis. CT-guided PTNB should be considered due to a less invasive nature than open lung biopsy. Although the diagnosis of amyloidosis should be based on tissue biopsy, in our study, three times of PTNB showed negative results. Searching amyloid in

more than one tissue and using different methods can exclude the possibility for false positive and false negative results and gives an idea for the heaviness and spread of the process [9].

Nodular parenchymal amyloidosis does not require a specific treatment. The surgical resection may be required if a large nodule causes a mass or space-occupying effect [6, 10].

In conclusion, pulmonary nodular amyloidosis is a rare and usually localized disease that can mimic other pulmonary disorders, such as neoplastic and granulomatous processes. As such, this condition should be considered in the differential diagnosis of pulmonary nodules or masses.

References

1. Wechalekar AD, Gillmore JD, Hawkins PN. Systemic amyloidosis. Lancet 2016;387:2641–54.

2. Gillmore JD, Hawkins PN. Amyloidosis and the respiratory tract. Thorax 1999;54:444–51.

3. Thompson PJ, Citron KM. Amyloid and the lower respiratory tract. Thorax 1983;38:84–7.

4. Urban BA, Fishman EK, Goldman SM, Scott WW, Jones B, Humphrey RL, et al. CT evaluation of amyloidosis: spectrum of disease. Radiographics 1993;13:1295-308.

5. Milani P, Basset M, Russo F, Foli A, Palladini G, Merlini G. The lung in amyloidosis. Eur Respir Rev 2017;26.pii: 170046. doi: 10.1183/16000617.

6. Zhang LN, Xue XY, Wang N, Wang JX. Mimicking pulmonary multiple metastatic tumors: A case of primary nodular parenchymal pulmonary amyloidosis with review of the literature. Oncol Lett 2012;4:1366-70.

7. Merino-Angulo A, Pérez-Martí M, Díaz de Otazu R. Pulmonary alveolar phospholipoproteinosis associated with amyloidosis. Chest 1990;98:1048.

8. Seo JH, Lee SW, Ahn BC, Lee J. Pulmonary amyloidosis mimicking multiple metastatic lesions on F-18 FDG PET/CT. Lung Cancer 2010;67:376–9.

9. Bogov B, Lubomirova M, Kiperova B. Biopsy of subcutaneus fatty tissue for diagnosis of systemic amyloidosis. Hippokratia 2008;12:236–9.

10. Lee SC, Johnson H. Multiple nodular pulmonary amyloidosis. A case report and comparison with diffuse alveolar-septal pulmonary amyloidosis. Thorax 1975;30:178–85.

11. Czeyda-Pommersheim F, Hwang M, Chen SS, Strollo D, Fuhrman C, Bhalla S. Amyloidosis: Modern cross-sectional Imaging. RadioGraphics 2015;35: 1381–92.

12. Parmar H, Rath T, Castillo M, Gandhi D. Imaging of focal amyloid depositions in the head, neck, and spine: amyloidoma. AJNR Am J Neuroradiol 2010;31:1165–70.

Case Report

Renal complication of crizotinib:
Crizotinib-associated complex renal cyst

Warissara Jutidamrongphan, M.D.
Pimporn Puttawibul, M.D.
From Department of Radiology, Faculty of Medicine, Prince of Songkla University, Songkhla, Thailand.
Address correspondence to W.J. (e-mail: warissara.jut@gmail.com)

Abstract
Crizotinib is one of the first-generation tyrosine kinase inhibitors targeting anaplastic lymphoma kinase (ALK) and was recently found to be associated with the development of complex renal cysts with an inconclusive explanation up to this time. Hereby, we discuss the hypothesis of crizotinib-associated complex renal cyst development and coexisting renal impairment after initiation of the treatment in a 75-year-old man with ALK-positive non-small cell lung cancer whose complex renal cysts evolved after initiation and cessation of crizotinib treatment. The coexistence as renal impairment persisted even after switching from crizotinib to ceritinib.

Keywords: Crizotinib, Non-small cell lung cancer, Complex renal cyst, ALK inhibitor.

Introduction
Non-small cell lung cancer is the most common form of lung cancer, accounting for 85% of the cases. [1] It is commonly found at an advanced stage by the time of diagnosis. Therefore, systemic therapies take part in major roles as the treatment of choice [2,3]. Crizotinib is a first-in-class, oral, small-molecule tyrosine kinase inhibitor of anaplastic lymphoma kinase (ALK), ROS1 and c-MET kinases [4].

In randomized trials involving patients with ALK-positive advanced NSCLC (PROFILE 1007, PROFILE 1014, and PROFILE 1029), crizotinib has proved to be effective over the standard single-agent chemotherapy with pemetrexed or docetaxel in extending progression-free survival[5] and pemetrexed plus platinum chemotherapy in the previously untreated universal [4,6] and especially Asian patients [7]. Subsequently, it has been approved to be the standard treatment of advanced ALK-positive NSCLC in many countries.

Despite plenty of advantages, crizotinib consequently discloses several adverse effects including gastrointestinal complaints, visual disturbances, interstitial lung disease, impaired renal function, and complex renal cyst [5,7–13]. The development of such complex renal cysts, or so-called crizotinib associated renal cysts (CARCs), has been reported to be observed in 4% of patients treated with crizotinib [14], and showed more incidence, particularly in the Asian population [11,14,15]. The imaging features of this matter should be recognized and not be mistaken for new metastasis or disease progression. Therefore, we would like to introduce a case study of a patient in our center with ALK-positive NSCLC treated with crizotinib and later on, developed multiple bilateral complex renal cysts despite achieving a good therapeutic response.

Case study

A 75-year-old man was pathologically diagnosed with non-small cell adenocarcinoma of the left upper lung. His chest CT scan showed advanced primary lung cancer with pleural and mediastinal nodal metastases, at least stage IVa or T3N2M1, together with a few simple hepatic cysts but no renal lesion. According to an ALK gene rearrangement in his tumor proved by fluorescence in situ hybridization (FISH) and immunohistochemistry, he received crizotinib treatment as the first-line therapy one month later and achieved a good therapeutic response.

On the CT scan taken at 43 days after the initiation of crizotinib, bilateral complex cystic lesions, seen as the mixed solid-cystic component with the thick, enhancing wall, emerging in both kidneys together with diffuse esophagitis and a few esophageal ulcers, were discussed for the most likely cause of the crizotinib side effect. Therefore, crizotinib was ceased. There was no further investigation or invasive procedure needed at the time. After 22 days of supportive treatment for esophagitis and ulcers, the gastrointestinal side effect improved. Thus, crizotinib was continued for 57 more days. Meanwhile, bilateral complex cystic lesions progressed in size and number. More aggressive characteristics were depicted as conglomeration together with newly developed hyperdense internal content, measured about 40 HU, thick wall enhancement, invasion into right iliopsoas muscle and surrounding fat inflammation. Simultaneously, the renal function was also impaired noted as creatinine rising and GFR drop. Eventually, crizotinib was once again ceased. Considering the effective therapeutic response of ALK-targeted therapy in this patient, ceritinib, one of the second-generation ALK inhibitors, was chosen as an alternative therapy after cessation of crizotinib for 21 days. The course of development from CT findings can be seen in Figure 1.

The bilateral complex cystic lesions and surrounding inflammation had gradually regressed within 66 days after cessation of crizotinib. The primary lung cancer also showed partial response whereas the renal function remained progressively and permanently impaired. In this regard, ceritinib was terminated after 23 days of treatment. After all, the patient was deemed to developed chronic kidney disease. The ultrasonography of the kidneys at 206 days after cessation of crizotinib showed neither residual complex cyst nor obstructive uropathy. Only small-sized ones in both kidneys were evident in Figure 2. The stable simple hepatic cysts remained unchanged all along.

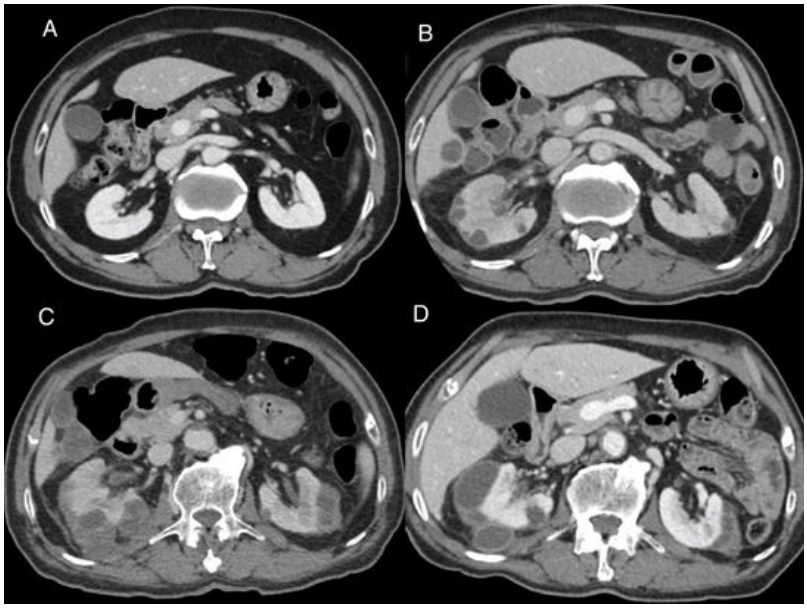

Figure 1: *Serial body CT scan revealed (A) No abnormal lesions before the introduction of crizotinib, (B) Development of bilateral complex cystic lesions at 43 days later. (C) Further growth of a complex cystic lesion extending from the right kidney to the iliopsoas muscle was still observed at 60 days after the first manifestation of bilateral complex cystic lesions. (D) The complex cystic lesion slightly decreased in size and showed less aggressive features at 66 days after cessation of crizotinib.*

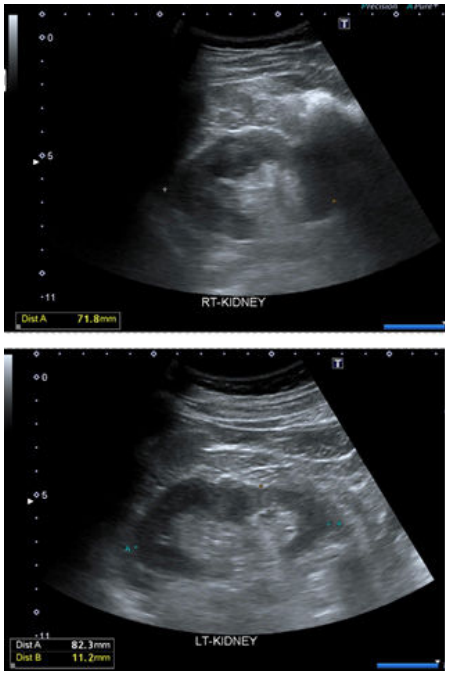

Figure 2: *Ultrasonography of the kidneys at 206 days after cessation of crizotinib revealed completely resolved complex cysts, left with only small-sized ones in both kidneys.*

Discussion

In the general population, renal cysts are deemed to be acquired from diverticula in distal convoluted and collecting renal tubules [16]. They are so common that over 50% of patients of more than 50 years old have at least one simple renal cyst [17,18]. Cystic lesions can be divided into simple and complex and accordingly categorized by Bosniak classification, based on computed tomographic characteristics. Some features, for instance, extensive calcification, septa with the irregular wall, thicker than 1 mm, solid portion, hyperdense fluid, irregular contour, contrast enhancement or evidence of inflammation separate complex from simple, benign cysts [19,20]. The categories IIF-IV correspond to complex cysts with increasing possibility of malignancy [11,13]. Crizotinib has been reported not only relating to the progression of existing renal cysts but also boosting the development of new renal cysts in the patients treated with crizotinib [12] with a higher incidence in the Asian population [12,18,21,22]. A series from Taiwan found evolved renal cysts in up to 22% of patients receiving this remedy [23]. As they usually develop septations or mixed cystic-solid appearances [15], the CARCs can also get complicated by rupture, infection and abscess formation [24,25], especially when prolonged neutropenia can also be a coexisting side effect of crizotinib[25], reported in about 9-14% of Crizotinib-treated patients participating in clinical trials [26]. They can even occur in conjunction with systemic inflammatory response, fever, and circulatory shock. Local extension into adjacent psoas muscle can also occur and require percutaneous drainage procedures to relieve the symptoms. However, most patients are usually able to continue crizotinib with only dose adjustment. Such aggressiveness together with complex features makes these CARCs mimicking metastatic disease and that makes it crucial to acknowledge this entity. Otherwise, patients could be misdiagnosed for infection or metastasis from lung cancer despite a good response of the primary lung cancer [27]. In order to differentiate between a malignant and benign lesions in most cases, positron emission tomography (PET) is proved to be useful by observing fluorodeoxyglucose (FDG) uptake. This process indicates abnormally increased metabolic activity and suggests more of the malignant origin. The CARCs,

unfortunately, have been reported to show FDG uptake as well[28] in spite of the aspiration and biopsy results showing benign xanthogranulomatous inflammation with negative bacterial culture and no evidence of malignant cell from the cytology [15].

Many patterns of CARCs progression have been described in the past decade. The most well-known pattern is that the renal cyst has shrunk after discontinuation of crizotinib or changing to alectinib [7,22,28]. The symptoms of coexisting systemic inflammation also improved after switching the medication [28]. However, there are also those whose CARCs shrank despite continued treatment with crizotinib and achieved a good therapeutic goal. Therefore, the degree of complexity of CARCs has reportedly no correlation with the malignant potential [12]. In our case study, the CARCs progressed within 43 days after the first cycle of crizotinib treatment and started to regress within 66 days after cessation of crizotinib.

The exact mechanism of CARCs is yet to be elucidated. Crizotinib is the first clinically available inhibitor of several tyrosine kinase receptors including ALK, c-MET and c-ROSC oncogene 1 [29]. Two main hypotheses have been proposed for the explanation, relating to hepatocyte growth factor and MET pathway (HGF-MET pathway) or testosterone levels. MET and HGF, which is a ligand of the MET receptor, are known to promote cystogenesis [7,30]. The usage of crizotinib causing inhibition of c-MET should cause cyst regression but the result is paradoxical. Yasuma et al [7] concluded in the recent study comprised of an in vivo experiment in mice. They suggested that there was no evidence of significant activation of Mapk/Erk or Stat3 pathway which was the HGF-mediated activation in the mice treated with crizotinib. The second hypothesis was depicted in the preclinical studies investigating the correlation between testosterone and polycystic kidney disease. The testosterone levels were found to influence the progression of renal cystic change in male and female rats with autosomal dominant polycystic kidney disease (ADPKD) [31,32]. Therefore, the imbalance of gonadal hormones may play some roles in the development of the complex renal cyst[25]. Crizotinib has been found to reduce testosterone

levels in patients with such levels returning to normal after discontinuance of Crizotinib [33]. This hypothesis provides opportunities for future researchers to explore its possibility.

Together with CARCs, renal impairment is one of the side effects of crizotinib which our case study also confronted. The study from the University of Colorado mentioned the reversible decrease of mean GFR by 23.9% compared to baseline in the first 2 weeks of therapy and that 84% of the patients recovered renal function after the cessation of therapy [23,34]. It was thought to be due to a defect in tubular excretion of creatinine rather than an actual drop in GFR. However, in the FAERS analysis, 88 cases of renal impairment were also noted [35]. Yasuma et al [7] again proposed that fibrosis and impaired renal function of the mice's kidneys during crizotinib therapy may be explained by blockade of the protective and anti-fibrotic activity of the HBF-c-MET pathways in the kidneys causing high mRNA expression of collagen I, abnormal glomerular expansion and increased interstitial collagen deposition.

In general, esophageal disorders like esophagitis, ulcer or reflux esophagitis were reported in about 20% of the 255 patients, but only 11% were attributed to crizotinib [36]. The coexisting diffuse esophagitis and a few esophageal ulcers had completely improved after supportive treatment despite the aggressive development of the bilateral renal cysts, which progressed in the same direction as a few previous case reports mentioned. The mechanism of the gastrointestinal side effect is still not well demonstrated. While Camidge et al [8] mentioned the role of ALK in the development of guts of other organisms, the exact function of the ALK is not well-known in humans. The recent study also suggested that the predominance of gastrointestinal side effects may be due to the anti-ALK effects in these tissues [37].

The coexisting hepatic cyst has also been reported to evolve together with the CARCs, regarding the aforementioned hypothesis [11,38]. However, our case study revealed no coincident complex feature development of the stable hepatic cyst in the baseline and follow-up CT, seen in Figure 3.

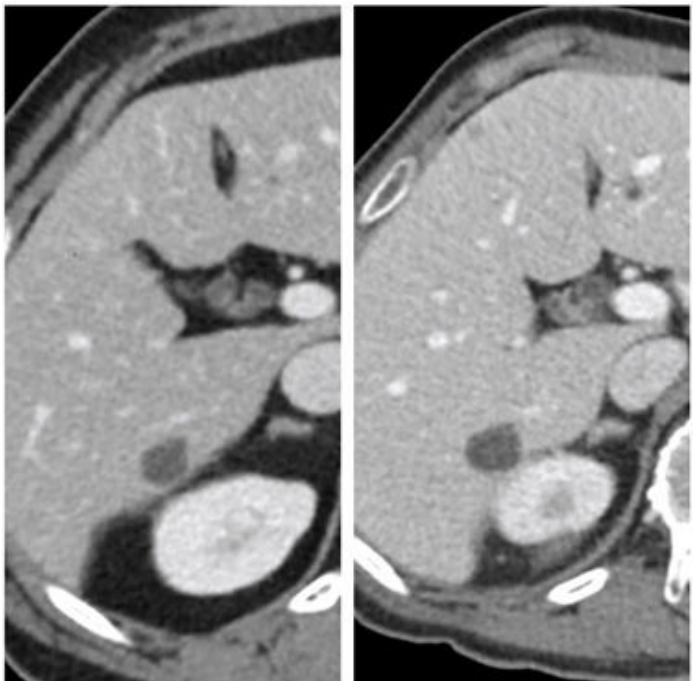

Figure 3: *Stable hepatic cyst on the baseline CT compared with the follow-up CT at 43 days after the initiation of crizotinib*

In conclusion, knowledge and prompt recognition of CARCs may help avoid the unnecessary invasive procedure, such as biopsy or drainage, and suboptimal treatment of lung cancer.

References

1. Dela Cruz CS, Tanoue LT, Matthay RA. Lung cancer: epidemiology, etiology, and prevention. Clin Chest Med 2011; 32:605-44.

2. Binder D, Hegenbarth K. Emerging options for the management of non-small cell lung cancer. Clin Med Insights Oncol 2013;7:221-34.

3. Ettinger DS, Bepler G, Bueno R, Chang A, Chang JY, Chirieac LR, et al. Non-small cell lung cancer clinical practice guidelines in oncology. J Natl Compr Canc Netw 2006;4:548-82.

4. Nishio M, Kim DW, Wu YL, Nakagawa K, Solomon BJ, Shaw AT, et al. Crizotinib versus chemotherapy in Asian patients with ALK-positive advanced non-small cell lung cancer. Cancer Res Treat 2018;50:691-700.

5. Shaw AT, Kim DW, Nakagawa K, Seto T, Crinó L, Ahn MJ, et al. Crizotinib versus chemotherapy in advanced ALK-positive lung cancer. N Engl J Med 2013; 368:2385-94.

6. Solomon BJ, Mok T, Kim DW, Wu YL, Nakagawa K, Mekhail T, et al. First-line crizotinib versus chemotherapy in ALK-positive lung cancer. N Engl J Med 2014;371:2167-77.

7. Yasuma T, Kobayashi T, D'Alessandro-Gabazza CN, Fujimoto H, Ito K, Nishii Y, et al. Renal Injury during Long-Term Crizotinib Therapy. Int J Mol Sci 2018;19:pii:E2902. doi: 10.3390/ijms19102902.

8. Camidge DR, Bang YJ, Kwak EL, Iafrate AJ, Varella-Garcia M, Fox SB, et al. Activity and safety of crizotinib in patients with ALK-positive non-small-cell lung cancer: updated results from a phase 1 study. Lancet Oncol 2012;13: 1011–9.

9. Di Girolamo M, Paris I, Carbonetti F, Onesti EC, Socciarelli F, Marchetti P. Widespread renal polycystosis induced by crizotinib. Tumori 2015;101:e128–31. doi: 10.5301/tj.5000338.

10. Heigener DF, Reck M. Crizotinib. In: Martins UM, editor. Small molecules in oncology. Berlin: Springer; 2014. p. 197–205.

11. Lin YT, Wang YF, Yang JC, Yu CJ, Wu SG, Shih JY, et al. Development of renal cysts after crizotinib treatment in advanced ALK-positive non-small-cell lung cancer. J Thorac Oncol 2014;9:1720–5.

12. Schnell P, Bartlett CH, Solomon BJ, Tassell V, Shaw AT, de Pas T, et al. Complex renal cysts associated with crizotinib treatment. Cancer Med 2015;4:887–96.

13. Souteyrand P, Burtey S, Barlesi F. Multicystic kidney disease: a complication of crizotinib. Diagn Interv Imaging 2015;96:393-5.

14. XALKORI U.S. Physician prescribing information [Internet]. New York, Revised 2016 March. [Cited 2019 Jan 15]. Available from: http://labeling pfzercom/ShowLabeling aspx.

15. Cameron LB, Jiang DH, Moodie K, Mitchell C, Solomon B, Parameswaran BK. Crizotinib Associated Renal Cysts [CARCs]: incidence and patterns of evolution. Cancer Imaging 2017;17:7.

16. Baert L, Steg A. On the pathogenesis of simple renal cysts in the adult. A microdissection study. Urol Res 1977;5:103-8.

17. Tada S, Yamagishi J, Kobayashi H, Hata Y, Kobari T. The incidence of simple renal cyst by computed tomography. Clin Radiol 1983;34:437–9.

18. Klempner SJ, Aubin G, Dash A, Ou S-HI. Spontaneous regression of crizotinib-associated complex renal cysts during continuous crizotinib treatment. Oncologist 2014;19:1008–10.

19. Bosniak MA. The current radiological approach to renal cysts. Radiology 1986;158:1–10.

20. Jia JB, Lall C, Tirkes T, Gulati R, Lamba R, Goodwin SC. Chemotherapy-related complications in the kidneys and collecting system: an imaging perspective. Insights Imaging 2015;6:479–87.

21. Liaw CW, Palese M, Fabrizio LD. A complex renal cyst in a patient on crizotinib: case report. Urology 2019;131:21-3.

22. Okubo K, Sato A, Nakamoto K, Hatanaka Y, Isono M, Hatanaka M, et al. Bosniak category III renal cysts caused by crizotinib in an anaplastic lymphoma kinase gene-rearranged non-small cell lung cancer patient. Urology 2018;121:e3–4. doi: 10.1016/j.urology.2018.08.008.

23. Jhaveri KD, Wanchoo R, Sakhiya V, Ross DW, Fishbane S. Adverse renal effects of novel molecular oncologic targeted therapies: a narrative review. Kidney Int Rep 2016;2:108–23.

24. Chan WY, Ang MK, Tan DS, Koh WL, Kwek JW. Imaging features of renal complications after crizotinib treatment for non-small-cell lung cancer: a case report. Radiol Case Rep 2016;11:245–7.

25. Yoneshima Y, Okamoto I, Arimura-Omori M, Kimura S, Hidaka-Fujimoto N, Iwama E, et al. Infected complex renal cysts during crizotinib therapy in a patient with non–small cell lung cancer positive for ALK rearrangement. Invest New Drugs 2015;33:510–2.

26. Kim DW, Ahn MJ, Shi Y, De Pas TM, Yang PC, Riely GJ, et al. Results of a global phase II study with crizotinib in advanced ALK-positive non-small cell lung cancer (NSCLC). ASCO Meeting Abstracts [abstract]. J Clin Oncol 2012; 30(15 Suppl):7533.

27. Eiamprapaporn P, Mungwatthana N, Twinprai P, Sookprasert A, Chindaprasirt J, Ahooja A, et al. Crizotinib-associated renal cysts in anaplastic lymphoma kinase-positive lung cancer patients: A single-center experience. Urol Int 2019; Sep 3:1- 4. doi: 10.1159/000502664.

28. Taima K, Tanaka H, Tanaka Y, Itoga M, Takanashi S, Tasaka S. Regression of crizotinib-associated complex cystic lesions after switching to alectinib. Intern Med 2017;56:2321-4.

29. Christensen JG, Zou HY, Arango ME, Li Q, Lee JH, McDonnell SR, et al. Cytoreductive antitumor activity of PF-2341066, a novel inhibitor of anaplastic lymphoma kinase and c-Met, in experimental models of anaplastic large-cell lymphoma. Mol Cancer Ther 2007;6(12 Pt 1):3314-22.

30. Horie S, Kano M, Kawabe K, Mikami Y, Okubo A, Nutahara K, et al. Mediation of renal cyst formation by hepatocyte growth factor. Lancet 1994;344:789-91.

31. Jayapalan S, Saboorian MH, Edmunds JW, Aukema HM. High dietary fat intake increases renal cyst disease progression in Han: SPRD-cy rats. J Nutr 2000;130:2356–60.

32. Cowley BD Jr, Rupp JC, Muessel MJ, Gattone VH 2nd. Gender and the effect of gonadal hormones on the progression of inherited polycystic kidney disease in rats. Am J Kidney Dis 1997;29:265-72.

33. Weickhardt AJ, Rothman MS, Salian-Mehta S, Kiseljak-Vassiliades K, Oton AB, et al. Rapid-onset hypogonadism secondary to crizotinib use in men with metastatic nonsmall cell lung cancer. Cancer 2012; 118:5302-9.

34. Brosnan EM, Weickhardt AJ, Lu X, Maxon DA, Barón AE, Chonchol M, et al. Drug-induced reduction in estimated glomerular filtration rate in patients with ALK-positive non-small cell lung cancer treated with the ALK inhibitor crizotinib. Cancer 2014;120:664–74.
35. Jhaveri KD, Sakhiya V, Wanchoo R, Ross D, Fishbane S. Renal effects of novel anticancer targeted therapies: a review of the Food and Drug Administration Adverse Event Reporting System. Kidney Int 2016;90:706-7.

36. Srivastava N, VanderLaan PA, Kelly CP, Costa DB. Esophagitis: a novel adverse event of crizotinib in a patient with ALK-positive non-small-cell lung cancer. J Thorac Oncol 2013;8:e23–4. doi: 10.1097/JTO.0b013e31827e2451.

37. Jalil AA, Craig J, Bajaj R, Spurling T. Severe ulcerative esophagitis induced by crizotinib therapy. ACG Case Rep J 2014;1:82-4.

38. Halpenny DF, McEvoy S, Li A, Hayan S, Capanu M, Zheng J, et al. Renal cyst formation in patients treated with crizotinib for non-small cell lung cancer-incidence, radiological features and clinical characteristics. Lung Cancer 2017;106:33–6.

Pictorial Essay

Four pulse sequences necessary for liver MRI interpretation

Linda Pantongrag-Brown, M.D.
From Advanced Diagnostic Imaging Center, Ramathibodi Hospital, Bangkok, Thailand.
Address correspondence to L.P. (e-mail: lbrown800@gmail.com)

Keywords: Liver MRI, Pulse sequences, Liver mass.

MRI is the best imaging modality for detection and characterization of liver masses. There are multiple pulse sequences used in MRI and they can be confusing and difficult to understand. Therefore, four important pulse sequences are introduced in this article in order to simplify the seemingly complex pulse sequences, and allow general radiologists and clinicians of all specialties to approach MRI of liver masses with ease.

Pulse sequence 1: T1 inphase/outphase (Figure 1)

This sequence is used to determine fat content. If the image voxel contains both water and fat, the signal will enhance in the T1 inphase and decrease in the T1 outphase. Fatty liver, focal fatty infiltration, and fat-sparing lesions can be diagnosed with this pulse sequence.

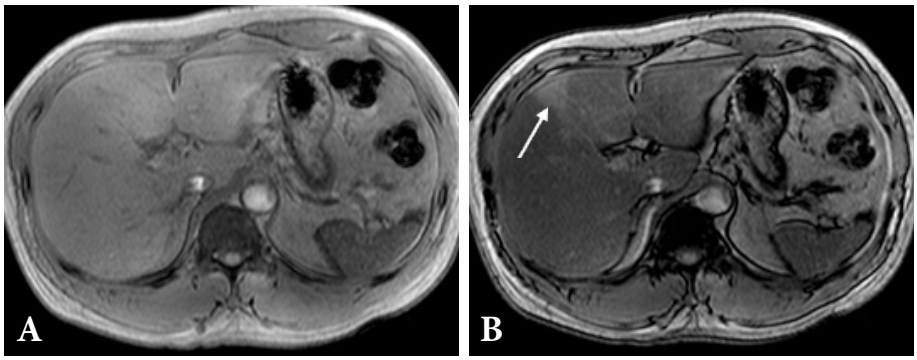

Figure 1: T1 inphase/outphase sequence
Fatty liver shows signal dropping at T1 outphase (B), compared to T1 inphase (A), except for an area of focal fatty sparing (arrow in B).

Pulse sequence 2: T2 and heavy T2 fat saturation (Figure 2)

T2 fat saturation (T2 FS) is a pulse sequence to determine if the lesion is a true or pseudo lesion. Most true lesions will exhibit high signal intensity (SI); exceptions exist, such as early hepatocellular carcinoma and focal nodular hyperplasia, which may show similar intensity to the liver. Heavy T2 is used to distinguish solid from cystic lesions and hemangiomas. Cysts and hemangiomas will show very bright SI, similar to spinal fluid, whereas solid lesions will show not-so-bright SI but just a higher signal than that of liver parenchyma.

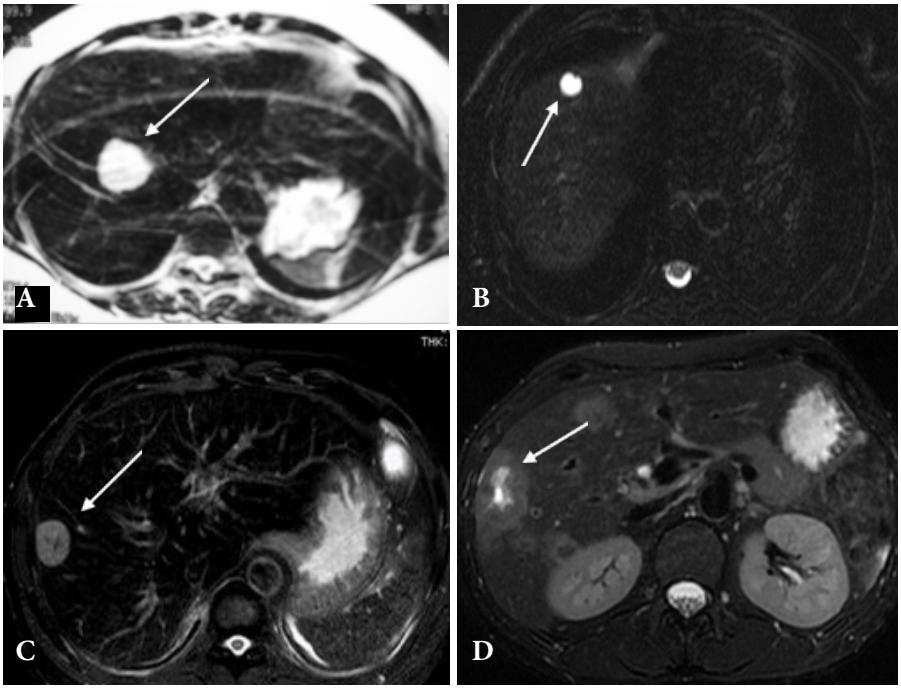

Figure 2: T2 and heavy T2 fat saturation sequence

Liver hemangioma (A), and liver cyst (B) show very bright SI at T2, whereas hepatoma (C) and metastasis (D) show not-so-bright SI, but just a higher signal than the liver parenchyma.

Pulse sequence 3: T1 dynamic gadolinium (Figure 3)

This is the most important pulse sequence for liver mass analysis. Vascular enhancement pattern is the key to characterizing each mass. Dynamic contrast study, with arterial, venous and delayed phases, is mandatory for the evaluation. Each tumor has its own characteristic pattern of vascular enhancement, although overlapping may occur.

If gadoxetic acid (Primovist), the hepatobiliary-specific contrast agent, is used, a 20 min delayed phase has to be evaluated after the dynamic phases. The liver parenchyma needs about 10-20 min to uptake contrast media and exhibit high SI. Most tumors show no uptake of gadoxetic acid. Generally, uptake of gadoxetic acid by a liver mass indicates benign nature. For example, uptake is seen with focal nodular hyperplasia (FNH), nodular regenerative hyperplasia (NRH), benign regenerating and low-grade dysplastic nodules.

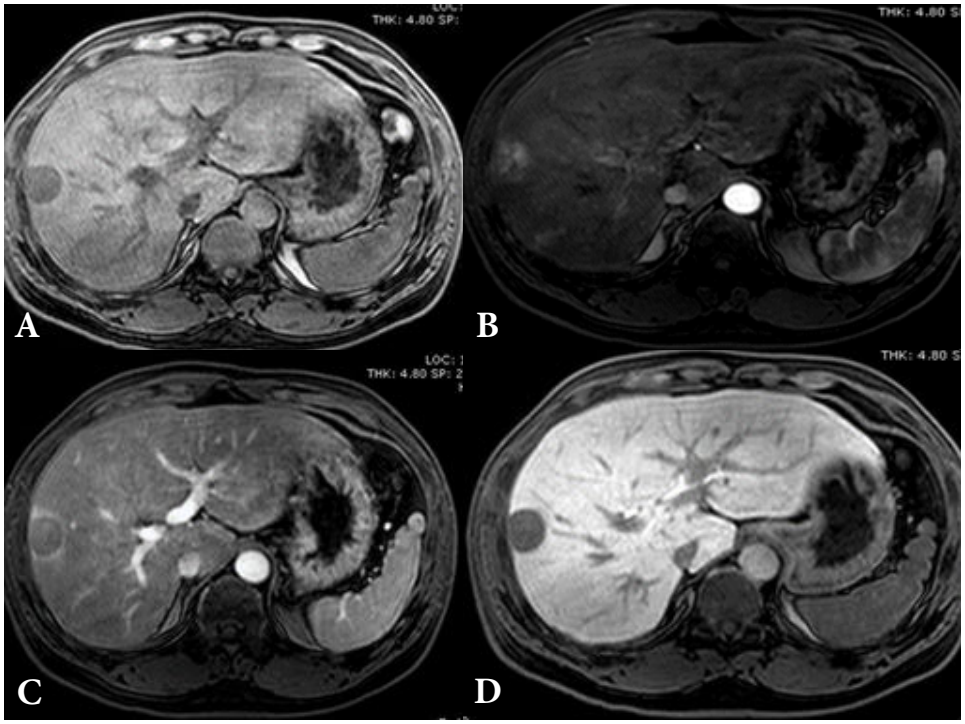

Figure 3: T1 dynamic gadoxetic acid contrast with 20 min delayed hepatobiliary (HB) phase of a small hepatocellular carcinoma

A: Pre-contrast shows a low SI nodule.

B: Arterial phase shows rapid enhancement of the nodule.

C: Venous phase shows rapid washout of the nodule.

D: 20 min HB phase shows no uptake of gadoxetic acid by the nodule. Note that the liver parenchyma shows high SI which is secondary to uptake of gadoxetic acid by normal hepatocytes.

Pulse sequence 4: Diffusion weighted image (Figures 4-5)

Diffusion weighted image (DWI) is a complimentary pulse sequence and not necessary for analyzing liver masses. It is based upon measuring the random Brownian motion of water molecules within a voxel of tissue. The relationship between histology and diffusion is complex. In general, highly cellular tissues or those with cellular swelling exhibit lower diffusion coefficients, and thus show abnormal fluid restriction. A low B value is sensitive but not specific, whereas a high B value is specific but not sensitive. Therefore, low and high B values are used in abdominal MRIs (B 0-50 for low, and B 500-1000 for high). DWI is a T2-based image, therefore T2 shine-through effect may mimic abnormal fluid restriction. When in doubt, combining with an ADC map is recommended. T2 shine-through effect will produce high ADC value, whereas true restriction will produce low ADC value.

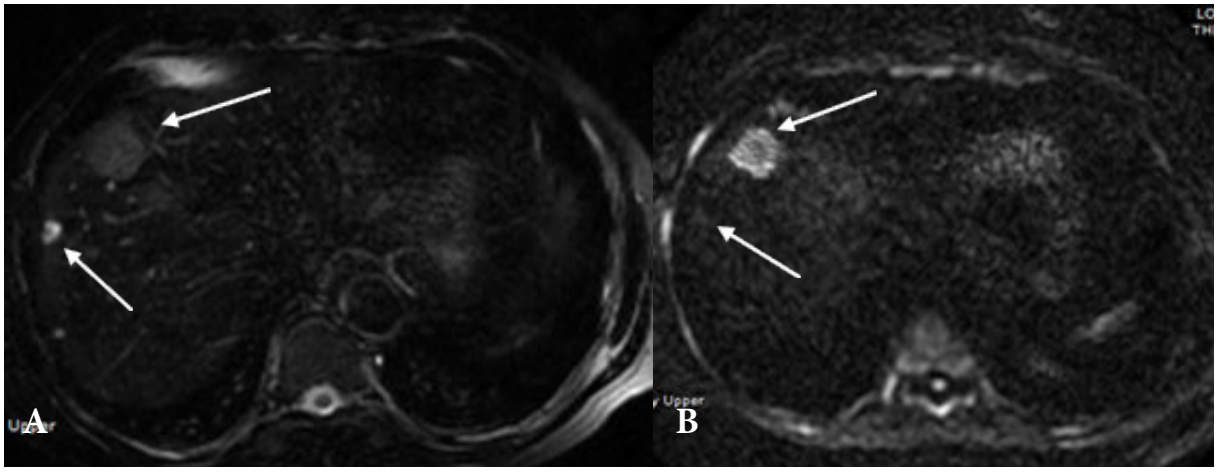

Figure 4: Diffuse weighted image (DWI), B 1000

Two lesions in the liver are demonstrated. The large nodule is a metastatic nodule, and the small nodule is a simple cyst. The large, metastatic nodule shows slightly high SI at T2 (A) with fluid restriction at DWI (B: seen as high SI). The small, simple cyst shows very high SI at T2 without fluid restriction at DWI (B: seen as isointense to the liver).

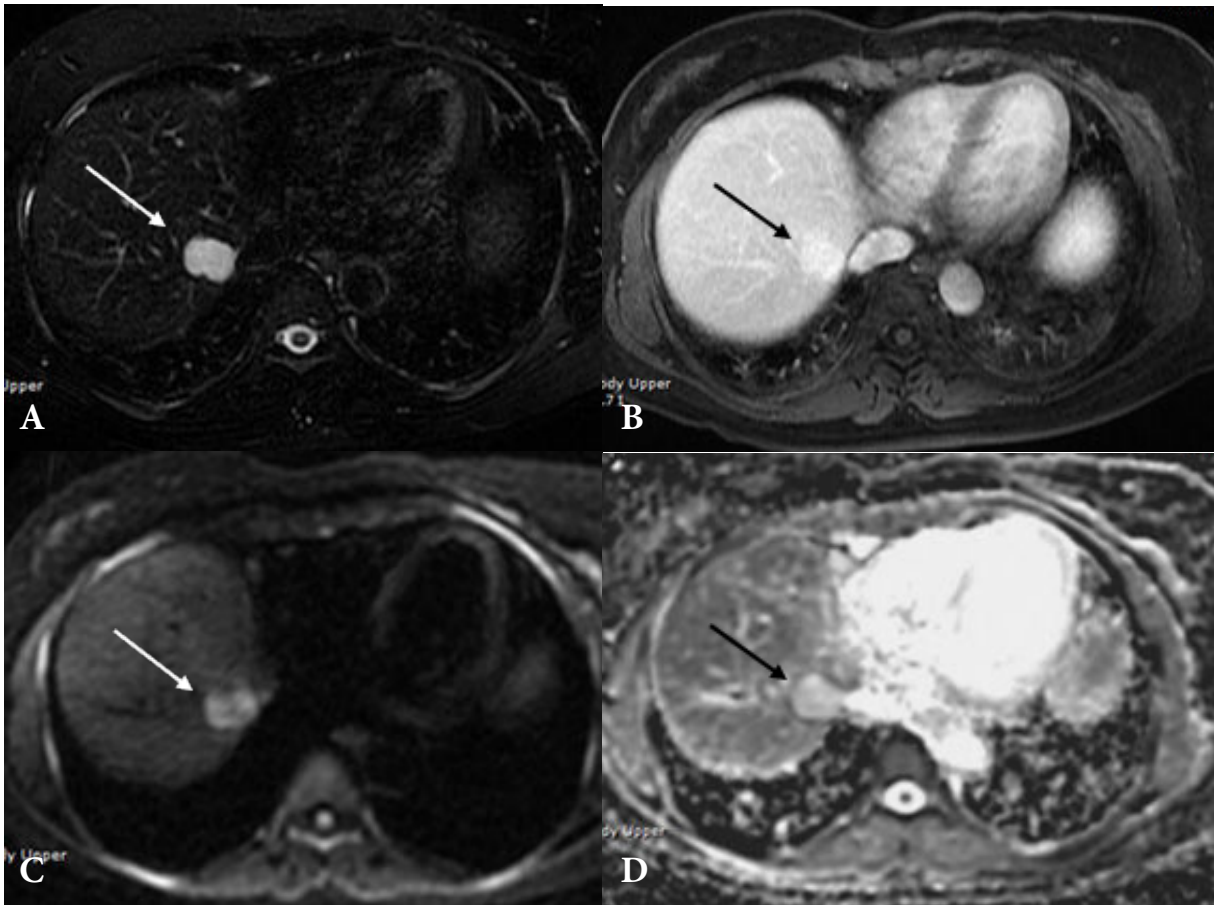

Figure 5: DWI and T2 shine-through effect
A hemangioma shows very high SI at T2 FS (A), and persistent enhancement in the delayed phase of contrast enhancement (B). At DWI (B 1000), the nodule shows high SI because of T2 shine-through effect (C), which is confirmed by high SI in the ADC map (D).

Case Examples

Following are examples of common liver lesions and the application of the above-mentioned pulse sequences for analysis. Each liver nodule, mass, and pseudo lesion exhibit a different MRI pattern [1-7]. Images of the lesions are shown and MRI patterns are interpreted using the summarized guidelines below.

1. Focal fatty infiltration (Figure 6)

MRI signal	Interpretation
T1 inphase/outphase	Signal loss = fat
T2 FS	Low SI = pseudo lesion
T1 dynamic gadolinium	No enhancement, normal vessels coursing through

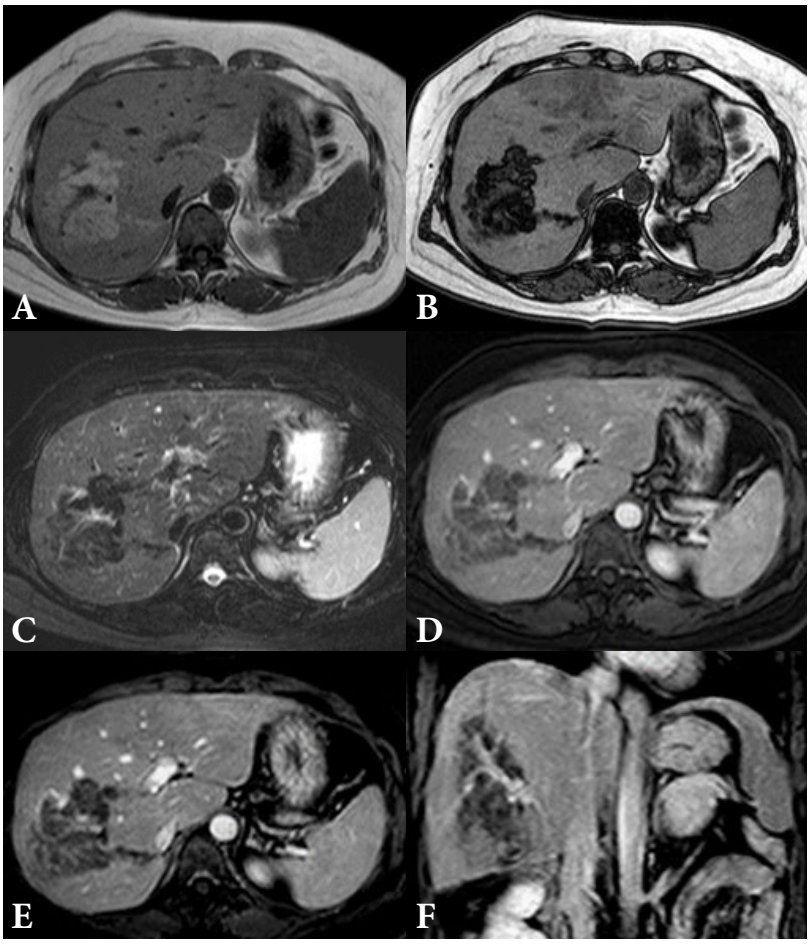

Figure 6: Focal fatty infiltration in an asymptomatic female
A, B: T1 inphase (A), and outphase (B) show a lobulated mass at right hepatic lobe with signal loss, indicative of a fat containing mass.
C: T2 FS shows the lesion to be low SI, suggestive of a pseudo lesion.
D-F: Arterial (D), venous (E), and delayed (F) phases show no enhancement within the lesion. Note the vessel coursing through this pseudo lesion, which is diagnostic for focal fatty infiltration.

2. Hemangioma (Figure 7)

MRI signal	Interpretation
T1 inphase/outphase	No signal loss = no fat
T2 FS	High SI = true lesion, very bright signal similar to spinal fluid
T1 dynamic gadolinium and 3 min delay	Peripheral nodular enhancement, central filling-in, and persistent enhancement throughout delayed phase

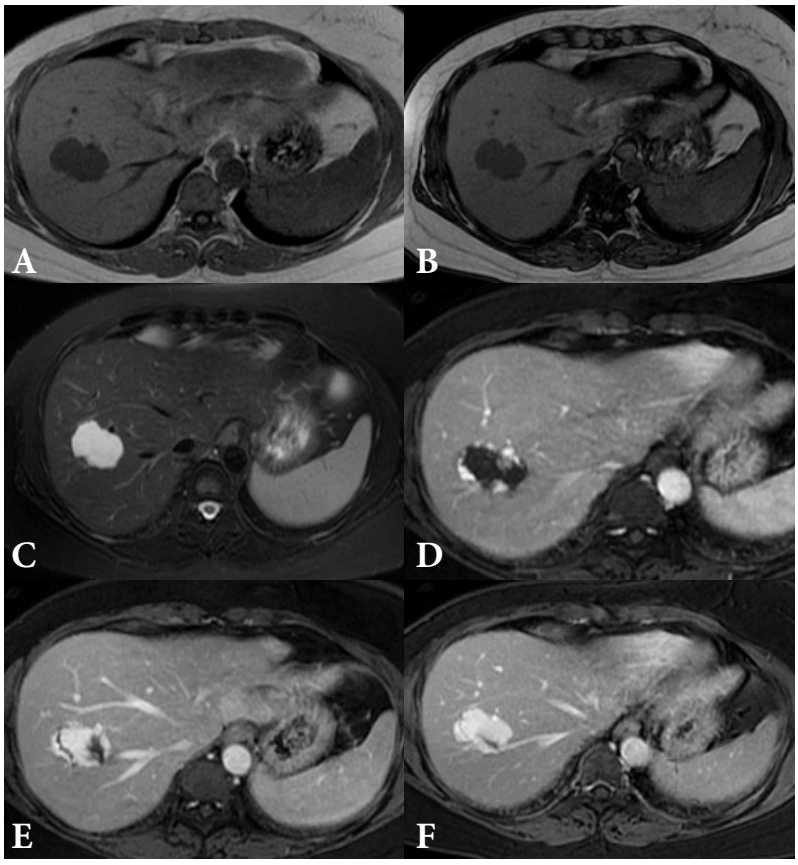

Figure 7: Hemangioma in a woman with breast cancer
A, B: T1 inphase/outphase shows a low SI nodule in the right hepatic lobe.
C: T2 FS shows the nodule to be high SI, similar to spinal fluid.
D-F: The nodule shows peripheral nodular enhancement at arterial phase (D), central filling-in at venous phase (E), and persistent enhancement throughout delayed phase (F). MRI pattern is characteristic of a benign hemangioma.

3. Focal nodular hyperplasia (Figure 8)

MRI signal	Interpretation
T1 inphase/outphase	No signal loss = no fat
T2 FS	High SI = true lesion, bright central scar
T1 dynamic and 20 min HB phase of gadoxetic acid contrast	Rapid arterial enhancement, retention of contrast, and uptake of gadoxetic acid

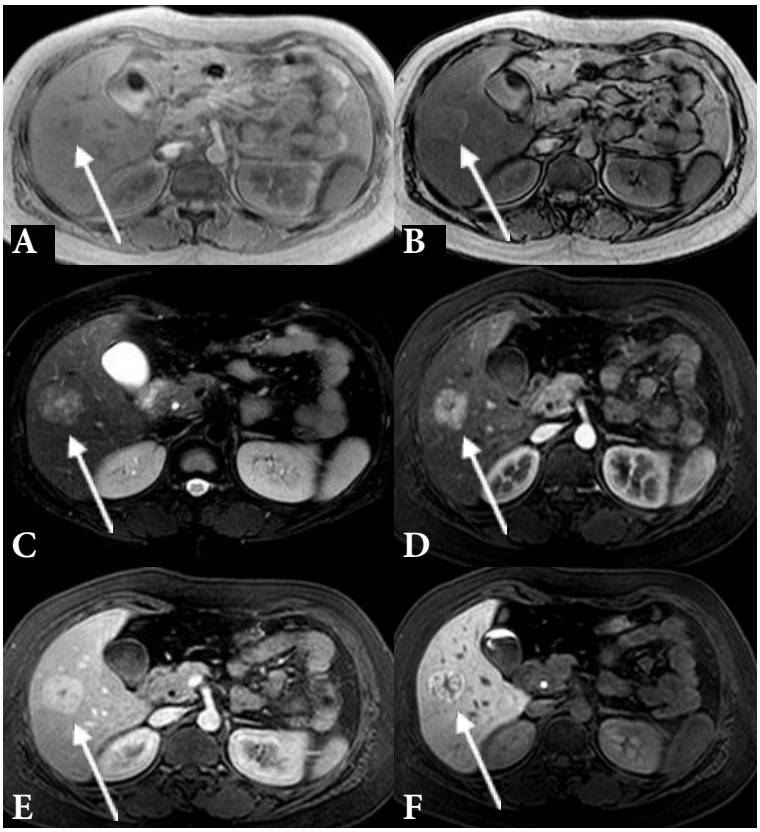

Figure 8: Focal nodular hyperplasia (FNH) in an asymptomatic woman

A, B: T1 inphase/outphase show fatty liver, as demonstrated by signal loss at outphase (B) compared to inphase (A). A lobulated mass at right hepatic lobe is noted.

C: T2 FS shows the nodule to be high SI with a very bright small central scar.

D-F: The nodule shows rapid arterial enhancement (D), retention of contrast at venous phase (E), and uptake of gadoxetic acid at HB phase [except for a central scar (F)]. This MRI pattern is characteristic of a benign FNH.

4. Hepatocellular carcinoma (Figure 9)

MRI signal	Interpretation
T1 inphase/outphase	No signal loss = no fat
T2 FS	High SI = true lesion
T1 dynamic and 20 min HB phase of gadoxetic acid contrast	Rapid arterial enhancement, rapid venous washout, and no uptake of gadoxetic acid
DWI ADC map	High SI = fluid restriction Low SI = confirms fluid restriction

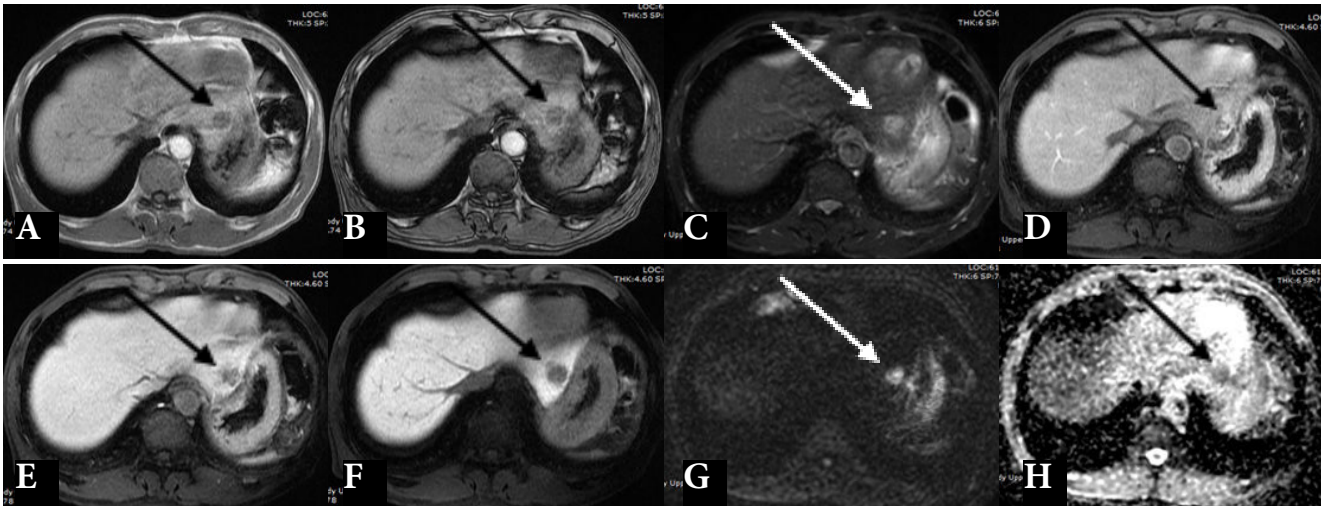

Figure 9: HCC in a man with chronic hepatitis B

A, B: T1 inphase/outphase show a 1.6 cm nodule at segment 2 of the left hepatic lobe.

C: T2 FS shows the nodule to be high SI, but not as bright as fluid.

D-F: The mass shows rapid arterial enhancement (D), rapid venous washout (E), and no uptake of gadoxetic acid contrast (F). This MRI pattern is characteristic of HCC.

G-H: The mass shows high SI at DWI, B 1000 (G) and low SI at ADC map (H), confirming the diagnosis of HCC.

Conclusions

1. MRI of the liver can be simplified in 4 key pulse sequences. Four key MRI pulse sequences are T1 inphase/outphase, T2 and heavy T2 FS, T1 dynamic gadolinium with 20 min HB phase (if gadoxetic acid contrast is used), and DWI.
2. T1 inphase/outphase is to determine fat content.
3. T2 is to differentiate true lesion from pseudo lesion.
4. T1 dynamic gadolinium is to determine vascular enhancement patterns. This is the most important pulse sequence. 20 min HB phase of gadoxetic acid is used to confirm a diagnosis of FNH, and to distinguish a dysplastic nodule from HCC.
5. DWI is a complimentary pulse sequence. A nodule with a highly cellular component usually shows fluid restriction at DWI.

References

1. Buetow PC, Pantongrag-Brown L, Buck JL, Ros PR, Goodman ZD. Focal nodular hyperplasia of the liver: radiologic-pathologic correlation. Radiographics 1996;16:369-88.

2. Hussain SM, Terkivatan T, Zondervan PE, Lanjouw E, de Rave S, Ijzermans JN, et al. Focal nodular hyperplasia: findings at state-of-the-art MR imaging, US,CT, and pathologic analysis. Radiographics 2004;24:3-9.

3. Pantongrag-Brown L. Imaging of focal liver masses. Thai J Gastroenterol 2004;5:130-6.

4. Pantongrag-Brown L. Multiple faces of focal nodular hyperplasia. Thai J Gastroenterol 2007;8:139-43

5. Pantongrag-Brown L. Imaging approach to liver mass. Part 1: Incidental finding without underlying liver disease. Thai J Gastroenterol 2008;9:43-7.

6. Pantongrag-Brown L. Imaging approach to liver mass. Part 2: Liver mass with underlying chronic liver disease. Thai J Gastroenterol 2008;9:113-6.

7. Anderson SW, Kruskal JB, Kane RA. Benign hepatic tumors and iatrogenic pseudotumors. Radiographics 2009;29:211-29. doi:10.1148/rg.291085099.

ASEAN Movement in Radiology

Sonographer school, HRH Princess Chulabhorn College of Medical Science: The first step of the sonographer system in Thailand

Surachate Siripongsakun, M.D.
From Sonographer School, HRH Princess Chulabhorn College of Medical Science, Chulabhorn Royal Academy, Bangkok, Thailand.
Address correspondence to S.S. (e-mail: surachate@yahoo.com)

Keywords: Education, Sonographer school, Sonography, Ultrasonography, Ultrasound.

Ultrasound is a diagnostic imaging tool, which is convenient, inexpensive and it provides non-radiation exposure. Thus, it is commonly used in a real-time diagnostic method in almost all medical fields. Nowadays, medical technology is widely used along with much more advanced development and ultrasound is considered a medical disruptive technology that is expected to expand in a wider scale in the near future.

In Thailand, ultrasonography still requires specialized physicians, especially radiologists, and obstetricians, resulting in some limitations and non-real time with an increasing number of services and long waiting time of patients in government hospitals before examinations, which could delay diagnosis and treatments.

In various developed countries such as Europe, America, and Australia, the medical sonographer has been developed as a system for diagnostics and ultrasound imaging among specialized physicians to perform and do a preliminary report of the ultrasound imaging, resulting in much lower waiting and more efficiency in the diagnostic examination.

In ASEAN countries, most of the ultrasound studies are provided by medical doctors; therefore, sonography training is still limited for physicians. Only a few countries including Singapore, Malaysia, and Thailand have formal training institutes for non-physician healthcare personnel at the level of post-graduate training, to provide formal sonography education/training to non-physician healthcare professions.

Basic information about the programs is provided in the table below (Table 1).

Table 1: Basic information of sonographer institutes in ASEAN region

Country	Singapore	Malaysia	Thailand
Institute	Singapore Institute of Technology, Singapore	Vision College, Selangor, Malaysia	Sonographer School, Princess Chulahborn College of Medical Science Bangkok, Thailand
Programs offer	Post graduate certificate in sonography, Post graduate diploma in sonography	Post graduate diploma of medical ultrasonography	Post graduate diploma in medical sonography, Master degree in medical sonography
Established since	No available online data	2005	2018
Affiliation	No available online data	University of South Australia, Adelaide, Australian Society of Ultrasound in Medicine	Monash University, Melbourne, Australia
Clinical modules provided	Abdominal sonography Pelvic Sonography Obstetric Sonography Small parts Sonography Vascular Sonography Musculoskeleton Sonography Neonatal and Paediatric Sonography	Abdominal sonography Obstetric and Gynecology Sonography Small parts Sonography Vascular Sonography Musculoskeleton Sonography Paediatric Sonography	Abdominal sonography Reproductive Sonography Obstetric Sonography Breast and thyroid Sonography Vascular and post operative Sonography Musculoskeleton Sonography
Souces	https://sitlearn.singaporetech.edu.sg/	https://www.vision.edu.my/	http://sonoschool.pccms.ac.th/

"Chulabhorn Royal Academy" is a government educational institution founded and named by Professor Dr. HRH Princess Chulabhorn Krom Phra Srisavangavadhana. Due to the awareness of the importance of this personnel development, the establishment of a medical ultrasound school was thus approved. On 1 June 2016, the committee for the Sonographer School establishment, led by Professor Dr. Jiraporn Laothammatat as the school chairman, agreed to collaborate with Monash University, a well-known and recognized institution for the sonographer curriculum, following the coordination by Assoc. Prof. Dr. Napapong Pongnapang, the vice president of ISRT (Asia Pacific region), who knew some instructors and the Head of Radiation Technology Department very well.

Then, Chulabhorn Royal Academy and Monash University entered a signed MOU for the sonographer curriculum development and collaboration on June 30, 2017 (Figure 1). After that, on October 4-9, 2017, the Sonographer School and Monash University organized the program of "Train the Trainer" for the school's instructors so as to prepare them to teach sonographer courses. This program was officially the first to share and exchange knowledge and experiences in ultrasonography between the two institutions.

Figure 1: *A signed MOU for the sonographer curriculum development and collaboration.*

On 1 December 2017, it was a very auspicious occasion that Professor Dr. HRH Princess Chulabhorn Krom Phra Srisavangavadhana proceeded to the ceremony for the official opening of the Sonographer School at Chulabhorn Chalermprakiet Medical Center Building, Lak Si District, Bangkok. It was the day of birth (Figure 2). The Sonographer School is the first sonographer school in Thailand, which initiated the admission of the 1st group of students in the Master of Science Program in Sonographer on August 1, 2018, onwards with Assistant Professor Dr. Surachate Siripongasakun as the first director of the school and the chairman of sonographer curriculum (Figure3).

Figure 2: *The official opening of the Sonographer School.*

Figure 3: *The first director of the school and the chairman of sonographer curriculum.*

The Sonographer School has opened many courses and programs for students as follows:

1. Master of Science Program in Medical Sonography
2. Postgraduate Diploma in Medical Sonography

   The Sonographer School is an educational institution that supports the study of ultrasonography at all levels, ranging from specialized physicians, general practitioners, radiologists, nurses, and other related medical science personnel, aiming to develop these medical personnel to use ultrasound technology for diagnosis and treatments with the increasing capacity of sonographers in order to provide fast and thorough ultrasound services.

Contact us

The Sonographer School, Faculty of Health Science Technology
HRH Princess Chulabhorn College of Medical Science, Chulabhorn Royal Academy

906 Kampangpetch 6 Road, Talad Bangkhen, Laksi, Bangkok 10210, Thailand
Tel. 66+02576-6000

Facebook: https://www.facebook.com/SonographerSchool/

ASEAN Movement in Radiology

Quality assurance in reading radiographs for pneumoconiosis: AIR Pneumo program

Naw Awn J-P M.D., Ph.D.
Narufumi Suganuma M.D., Ph.D.
From Department of Environmental Medicine, Kochi Medical School, Kochi University, Nankoku, Kochi, Japan.
Address correspondence to N.A. (e-mail: jpnawawn@kochi-u.ac.jp)

Conflict of Interest: The authors declare that they have no conflict of interest.

Keywords: Chest radiography, ILO classification system, Pneumoconiosis, Quality assurance, AIR Pneumo.

Background

Occupational exposures to various dusts are widespread and pneumoconiosis represents one of the major occupational lung diseases worldwide. Chest radiography is extensively used in the screening for pneumoconiosis in dust-exposed workers. However, recognition of early pneumoconiosis in a chest radiograph is difficult and interpretation is different among physicians. To achieve uniformity in interpretation, the International Labour Office has developed a standardized system for reading chest radiographs for the presence of pneumoconiosis (ILO Classification system) [1]. Despite the introduction of this classification system, inconsistency between readings exists among physicians as well as an individual physician. To improve consistency in readings and to

maintain physicians' proficiency in using the ILO Classification system, the National Institute for Occupational Safety and Health (NIOSH) of the United States has developed the B Reader Certification Program in 1974 [2]. This program provides training courses in the application of the ILO Classification system and administers examinations for certification. The B Reader Certification Program also opens to physicians from outside the United States; however, most physicians from developing countries have several constraints in accessing the benefits offered by the program.

Asian Intensive Reader of Pneumoconiosis (AIR Pneumo)

Back in 2003, a dialogue was developed between a government official of Thailand and Professor Yukinori Kusaka (School of Medicine, University of Fukui, Japan) about setting up an Asian certification program for reading chest radiographs for pneumoconiosis. Following this, a number of experts, all having backgrounds within occupational medicine, formed a working group, used their expertise to formulate the structure of the program. The team consisted of experts from across the world including Brazil, China, Germany, India, Japan, Thailand, the United States, and Viet Nam. During a series of workshops, the expert group made a great effort to develop a comprehensive training course and an examination program. Finally, in 2006, the Asian Intensive Reader of Pneumoconiosis (AIR Pneumo) (www.airp.umin.jp) was established as an academia-based quality assurance program for physicians' proficiency in reading chest radiographs for pneumoconiosis [3]. The objective was to upgrade the skills of physicians in developing Asian countries in reading chest radiographs for pneumoconiosis by using the ILO Classification system.

To fulfill its objective, AIR Pneumo provides a program involving training, examination, and certification to all physicians who are working to protect workers' health. AIR Pneumo program is driven by an international expert

committee. The committee members came from various disciplines including chest medicine, occupational medicine, public health, and radiology. Most importantly, all have the same interests in the prevention of pneumoconiosis. The training courses are designed as two days of lectures and practical exercises using examples chest radiographs [4]. The lectures include the epidemiology of dust-induced lung diseases, basic principles and quality in chest radiography, radiological findings consistent with dust-induced pulmonary and pleural lesions, and the application of the ILO Classification system in screening and surveillance for pneumoconiosis. The practical exercise sessions involve an interactive reading of representative chest radiographs of pulmonary and pleural lesions instructed by international experts. In the examination, candidates classify 60 chest radiographs. Performance in the examination is assessed by the accuracy in detecting parenchymal lesions consistent with pneumoconiosis, accuracy in detecting pleural lesions, and consistency in classifying shape and profusion of small opacities. A participant must pass the examination to receive the AIR Penumo Certification. To maintain their status, they must pass a recertification examination every five years.

ASEAN community countries and pneumoconiosis

For the first time in 2014, a conference for cooperation among ASEAN community countries to improve the proficiency in reading chest radiographs for pneumoconiosis according to the ILO Classification system was organized in Chiangmai, Thailand. ("ASEAN Conference for the Development of National Readers for ILO Classification" Project of Cooperation among ASEAN Community Countries to improve the diagnosis and proficiency in Reading Pneumoconiosis Chest Radiographs According to ILO Classification, 28-30 July 2014, Chiangmai, Thailand.) Officials from eight ASEAN community countries including Brunei, Cambodia, Indonesia, Laos, Malaysia, the Philippines, Thailand, and Vietnam presented in the conference. The national as well as regional situation in the epidemiology, prevention and control of pneumoconiosis were discussed. The following facts are derived from the conference:

1. The estimated dust-exposed workers ranged from 40,000 to 1.6 million across the ASEAN countries. The major occupation included construction, coal mining, quarries, stone carving, stone cutting and grinding, foundry, porcelain and ceramics, and sandblasting.

2. The estimated prevalence of pneumoconiosis ranged from 20% to 40% of the potential population. However, there were no established reporting and a data management system for pneumoconiosis across ASEAN countries.

3. In 2014, the number of dedicated occupational health physicians ranged from 8 to 500 across ASEAN countries. Generally, the diagnosis of pneumoconiosis is performed by chest physicians; however screening is conducted by occupational health physicians.

4. Only five ASEAN community countries (Indonesia, Malaysia, the Philippines, Thailand, and Vietnam) conducted training workshops (in collaboration with the ILO) to promote physicians' proficiency in the application of the ILO Classification system in the past. Only Thailand has qualified NIOSH B Readers.

5. All ASEAN community countries showed their interests in training national readers for pneumoconiosis.

The conference concluded that fostering physicians who are competent in reading chest radiographs for pneumoconiosis is central to the implementation of proper medical screening, and it is also important to the prevention of pneumoconiosis. The training programs could be organized through regional cooperation among ASEAN community countries along with collaborative supports from international organizations such as the ILO.

The ASEAN Conference for the Development of National Readers for ILO Classification: Project of Cooperation among ASEAN Community Countries to improve the diagnosis and proficiency in Reading Pneumoconiosis Chest Radiographs According to ILO Classification held in Chiang Mai, Thailand, 28-30 July 2014

The experts from Japan and the participants from eight ASEAN countries including Brunei, Cambodia, Indonesia, Laos, Malaysia, Philippines, Thailand, and Viet Nam.

The 1st conference was held in Chiang Mai in Northern Thailand.

Positioning of AIR Pneumo in pneumoconiosis prevention

To promote physicians' proficiency in reading chest radiographs for pneumoconiosis in developing Asian countries, the AIR Pneumo is working hard through international collaboration including the Asian Pacific Society of Respirology (APSR), the International Labour Office (ILO), the Scientific Committee on Respiratory Disorders of the International Commission on Occupational Health (ICOH SCRD), the Research Group for Occupational Lung Diseases of the Japan Society for Occupational Health (JSOH), the Research Group for International Cooperation in Occupational Health of the Association of Occupational and Environmental Diseases of Thailand (AOET), the Central Chest Institute of Thailand (CCIT), and the Bureau of Occupational and Environmental Diseases of the Ministry of Public Health of Thailand. Previously, the Central Chest Institute of Thailand was the only institution that could accommodate candidates for the AIR Pneumo training and examination programs. At the Central Chest Institute of Thailand, the program was conducted biennially and physicians from other Asian countries (such as Bhutan, Hongkong, India, Taiwan) participated. From 2018, AIR Pneumo, in collaboration with Universitas Indonesia-Persahabatan Hospital, Universitas Indonesia Hospital Depok, the Indonesian Society of Respirology (ISR) and the Indonesian Occupational Medicine Association, and expanded its training and examination program to Indonesia. Examination seats could be arranged for about forty number of candidates. By the end of 2019, AIR Pneumo has successfully conducted it's training and examination programs twenty two times in several countries: India, the Philippines, and Vietnam hosted once; Indonesia did so thrice, Brazil, and Japan organized it five times in each country, and Thailand held it for six times. The examination for AIR Pneumo certification was administered to 530 candidates, including 138 chest physicians, 150 occupational physicians, and 100 radiologists (see the table). Of the 530 physicians, 425 physicians received certifications for their competency in classifying chest radiographs for the presence of pneumoconiosis.

Physicians participated in the examinations for AIR Pneumo certificate, according to their country and specialty, n=530

	n	(%)
Country		
Brazila	48	(9.1)
India	58	(10.9)
Indonesia	140	(26.4)
Japan	47	(8.9)
Malaysia	15	(2.8)
Philippines	23	(4.3)
Thailand	128	(24.2)
Viet Nam	57	(10.8)
Othersb	14	(2.6)
Specialty (n=473)		
Chest medicine	138	(29.2)
General medicine	54	(11.4)
Occupational medicine	150	(31.7)
Public health	22	(4.7)
Radiology	100	(21.1)
Others	9	(1.9)
AIR Pneumo certified physicians	427	(80.6)

[a] *including physicians from Argentina, Chile, and Peru*
[b] *including physicians from Brunei, Cambodia, DR Congo, Hong Kong, Khindom of Bhutan, Myanmar, Parkistan, and Taiwan*

In 1995, the International Labour Organization and World Health Organization launched a Global Program on the Elimination of Silicosis (WHO/ILO GPES) [5]. The objective was to eliminate new cases of silicosis in all countries by 2030. In order to support the implementation of the ILO/WHO GPES, the AIR Pneumo is active in disseminating knowledge, educating physicians in reading radiographs for pneumoconiosis, and performing as a "special bridge" to promote relations and cooperation among Asian countries.

Acknowledgments

AIR Pneumo project consumed great amount of work, research, and dedication. Still, it's training and examination programs would not have been possible without supports from many individuals and organizations. Therefore, we would like to extend our sincere gratitude to all of them, but the list here is not exhaustive. First of all, we are grateful to Yukinori Kusaka (Emeritus Professor, University of Fukui, Japan; Former Chair, AIR Pneumo Project), Hisao Shida (Committee of Compensation of Asbestos-related Diseases, Ministry of the Environment, Japan), Masanori Akira (Department of Radiology, National Hospital Organization Kinki-Chuo Chest Medical Center, Japan), Taro Tamura (Fukui City Public Health Center, Japan), Somkiat Siriruttanapruk (Department of Disease Control, Ministry of Public Health, Thailand), Ponglada Subhannachart (Advisory Level, Central Chest Institute of Thailand), Sutarat Tungsagunwattana, MD (Central Chest Institute of Thailand), Xing Zhang (Zhejiang Academy of Medical Sciences, China), Prahalad K. Sishodiya (National Institute of Miners' Health, India), Tran Anh Thanh (Occupational Health Management Division, Ministry of Health, Viet Nam), Kurt G. Hering (Department of Diagnostic Radiology, Radio-oncology and Nuclear Medicine, Radiological Clinic, Miner's Hospital, Germany), John E. Parker (Pulmonary and Critical Care Medicine, Robert C. Byrd Health Sciences Center, School of Medicine, West Virginia University, USA), Eduardo Algranti (Divisao de Medicina, Fundacentro, Brazil), Agus Dwi Susanto (Department of Pulmonology and Respiratory Medicine, Faculty of Medicine, Universitas Indonesia), Muchtaruddin Mansyur (Occupational Medicine Division, Faculty of Medicine, Universitas Indonesia) for provision of expertise, and technical support to the project. Second, we would like to express our sincere thanks towards volunteer experts who devoted their time and knowledge in the training programs as lecturers. Finally, we express our gratitude toward all the participants of the AIR Pneumo training and examination programs.

Speakers and participants in the 5th AIR Pneumo Training Workshop in Thailand held in December 2016

Expansion of the project. More participants joining the 6th AIR Pneumo Training Workshop at Central Chest Institute of Thailand in December 2018

Closing ceremony and certificate presentation to the successful participants at the 6th and the latest AIR Pneumo Training Workshop in December 2018

Expansion of the project. The 2nd AIR Pneumo Training Workshop in Indonesia held in February 2019

References

1. International Labour Office. Guidelines for the use of the ILO International Classification of Radiographs of Pneumoconioses. Revised Edition 2000. Geneva: ILO; 2002.

2. CDC Centers for Disease Control and Prevention [Internet]. Atlanta, GA: The National Institute for Occupational Safety and Health; [updated 2019 March 4; cited 2019 November 15]. Chest Radiography: The NIOSH B Reader Program. Available from: https://www.cdc.gov/niosh/topics/chestradiography/breader.html.

3. Suganuma N, Natori Y, Kurosawa H, Nakano M, Kasai T, Morimoto Y, et al. Update of occupational lung disease. J Occup Health 2019;61:10-8.

4. Zhou H, Kusaka Y, Tamura T, Suganuma N, Subhannachart P, Siriruttanapruk S, et al. The 60-film set with 8-index for examining physicians' proficiency in reading pneumoconiosis chest X-rays. Ind Health 2012;50:84-94.

5. Fedotov IA, Eijkemans GJM. The ILO/WHO Global Programme for the Elimination of Silicosis (GPES). GOHNET Newsletter 2007;(12):1-3.

ASEAN

This journal provide 4 areas of editorial services: language editing, statistical editing, content editing, and complete reference-citation check in 8 steps:

Step	Services to Authors	Services providers
I	Manuscript submitted	Editor
II	Language editing/ A reference-citation check	Language Consultant/Bibliographer
III	First revission to ensure that all information remains correct after language editing	Editor
IV	Statictical editing	Statistical consultant
V	Content editing*	Two reviewers
VI	Second revision	Editor
VII	Manuscript Accepted/Rejected	Editor/Editorial board
VIII	Manuscript Published	Editorial office

*Content editing follows a double-blind reviewing procedure

JOURNAL OF RADIOLOGY